

PAPER

View Article Online
View Journal | View Issue



Cite this: *Environ. Sci.: Nano*, 2025, 12, 2667

A quality-by-design inspired approach to develop PET and PP nanoplastic test materials for use in *in vitro* and *in vivo* biological assays†

Lukas Wimmer, ^{ab} My Vanessa Nguyen Hoang, ^{ab} Jacqueline Schwarzingner, ^{ab} Vesna Jovanovic, ^c Boban Anđelković, ^d Tanja Cirkovic Velickovic, ^{cd} Thomas C. Meisel, ^{id e} Tassilo Waniek, ^f Christiane Weimann, ^f Korinna Altmann ^{id f} and Lea Ann Dailey ^{id *a}

Micro- and nanoplastics have become environmental pollutants of concern, receiving increased attention from consumers, scientists, and policymakers. The lack of knowledge about possible impacts on wildlife and human health requires further research, for which well-characterized test materials are needed. A quality-by-design (QbD) driven approach was used to produce sterile, endotoxin monitored nanoplastics of polyethylene terephthalate (PET) and polypropylene (PP) with a size fraction of >90% below 1 μm and high yield of >90%. Glycerol was used as a versatile and biocompatible liquid storage medium which requires no further exogenous dispersing agent and maintained colloidal stability, sterility (0 CFU mL^{-1}), and low endotoxin levels (<0.1 EU mL^{-1}) for more than one year of storage at room temperature. Further, the glycerol vehicle showed no biological effect on the tested human bronchial cell line Calu-3 up to 0.8% (w/v). Given the concentration of 40 mg g^{-1} nanoplastics in the glycerol stock, this corresponds to a nanoplastic concentration of 320 $\mu\text{g mL}^{-1}$. The surfactant-free nanoplastics are dispersible in bio-relevant media from the glycerol stock without changing size characteristics and are suitable for *in vitro* and *in vivo* research.

Received 19th December 2024,
Accepted 31st March 2025

DOI: 10.1039/d4en01186d

rsc.li/es-nano

Environmental significance

Micro- and nanoplastics have become environmental pollutants of concern with unknown implications for human health. To better understand the role of nanoplastics in this context, the spectrum of available and environmentally relevant test materials needs to be broadened beyond the commonly studied polystyrene beads. In-house nanoplastic production methods usually focus on particle size as the only property of interest and contain exogenous surfactants which can contribute to biological effects. Hence, there is a strong need to develop test materials that fulfill a broader spectrum of requirements needed for use in *in vitro* and *in vivo* biological assays.

Introduction

The problem of plastic pollution has been recognized by scientists since the 70s¹ and has garnered increasing interest

from policymakers^{2–4} and the general public⁵ in recent years. The growing production volume⁶ with a high share of single-use plastic and difficulties in recycling⁷ has led to a steady increase in plastic waste.⁸ Ultimately this plastic waste ends up in landfills,⁹ where its release into the environment cannot be avoided.¹⁰ Although synthetic polymers are very durable, they fragment^{11,12} under environmental conditions, even down to the nanoscale.^{13,14} To this day there is no consensus on the size nomenclature.^{15,16} However, there is a majority consensus around the definition provided by Hartmann *et al.* defining nanoplastics as non-fibrous particles with a diameter of 1 nm - 1 μm in the largest dimension.¹⁷ This definition was also adopted by policymakers in the EU,¹⁸ the International Organization for Standardization (ISO),¹⁹ and the World Health Organization (WHO).²⁰ Unsurprisingly, micro- and nanoplastics (MNPs)

^a Department of Pharmaceutical Sciences, University of Vienna, Vienna, Austria.
E-mail: leaann.dailey@univie.ac.at

^b Vienna Doctoral School of Pharmaceutical, Nutritional and Sport Sciences (PhaNuSpo), University of Vienna, Vienna, Austria

^c Department for Organic Chemistry, Faculty of Chemistry, University of Belgrade, Belgrade, Serbia

^d Serbian Academy of Sciences and Arts, Belgrade, Serbia

^e Department of General and Analytical Chemistry, Montanuniversität Leoben, Leoben, Austria

^f Bundesanstalt für Materialforschung und -prüfung (BAM), Berlin, Germany

† Electronic supplementary information (ESI) available. See DOI: <https://doi.org/10.1039/d4en01186d>



are ubiquitously present on the planet^{21–25} as their small size favors transport *via* aquatic^{26–28} and atmospheric^{29,30} mechanisms. Studies suggest that living organisms, including humans, can internalize MNPs,^{31–34} which raises concerns about human³⁵ and ecosystem³⁶ health impacts due to continuous exposure *via* food,^{37,38} water,^{39,40} air,^{41–43} and soil.^{28,44}

Despite intensive research efforts, the implications for human health are still unknown, primarily due to limitations in analytical methods and a lack of standardization. Well-characterized and standardized materials for calibration, validation and comparison studies are urgently needed.^{45–51} The development of such materials is supported by several guidance documents issued by the National Institute of Standards and Technology (NIST)⁵² and ISO.^{53–55} Test materials are categorized into four major groups dependent on the intended applications and level of characterization provided in the form of a suitable data and information sheet: 1) research grade test materials, 2) reference materials, 3) certified reference materials, and 4) standard reference materials (Table 1).

Currently, polystyrene (PS) beads are the only certified reference materials available in the nanoplastic size range (1 nm to 1 μ m). Table 2 provides a selection of commercially available test and reference materials, which illustrates that there is scope for broadening the spectrum of available materials for research purposes, especially regarding the number of polymer types. Furthermore, none of the research grade test and reference materials cited have been specifically validated for intended use as comparator materials in *in vitro* and *in vivo* biological assays. “Off label usage” as comparator materials in biological assays, such as toxicity tests, is widespread but not without limitations.^{57–60} For example, when reference materials are developed as instrument calibration standards, the addition of disclosed or undisclosed additives, such as surfactants for colloidal stability and preservatives to prevent microbial growth in aqueous preparations is common and unproblematic, since these additives do not negatively impact results generated within the context of the intended use. However, additives or surface modifications can be problematic for biological assays, as they may interfere with the assay or complicate

the interpretation of results.^{61–64} As a response, many groups have recently reported methodologies to prepare nanoplastic test materials in-house for use in biological assays.^{45,48,50,65} It is important to note that many of these studies focus primarily on particle size and surface charge as the defining material attributes.^{66–69} While these parameters are important, they are not the only criteria necessary for use in many biological assays.

In this study, we have implemented a quality-by-design (QbD)-inspired approach to develop polyethylene terephthalate (PET) and polypropylene (PP) nanoplastic test materials for intended use in *in vitro* and *in vivo* biological assays. QbD is a system used across a wide range of industries for product design and optimization. One of the primary pillars of the QbD approach is to define the intended use of a product and its desired properties at the very beginning of a development process. Hence, the product is specifically designed to meet the criteria for the intended use.⁷⁴ When applied to the development of nanoplastic test materials for use in biological assays, the QbD approach starts with the development of a target product profile (TPP) which describes the intended use and the desired product characteristics. In the current project, we would like to design nanoplastics suitable for use in cell-based assays, protein and/or eco-corona studies and *in vivo* toxicity tests. To be suitable for such applications, the test materials must fulfill all criteria described in Fig. 1.

Very few production methodologies described in the literature can satisfy these requirements. Nanoplastics produced as aqueous dispersions often require the addition of surfactants and preservatives, and are often only colloidally stable at low concentrations, which do not enable dose-escalation studies.^{49,50,66,75} To overcome these limitations, we explored glycerol as a biocompatible storage medium for our PET and PP research grade test materials. The rationale for our choice of glycerol as a non-aqueous storage medium included the following points:

- Glycerol is a non-volatile, natural preservative, maintaining microbial stability during storage at room temperature.⁷⁶
- The high viscosity of glycerol prevents agglomeration over long storage periods, even at high concentrations without exogenous surfactants.

Table 1 Test material categories and their definitions according to NIST and ISO

Category	Definition
Research grade test material (RGTM)	Exploratory materials developed for current research needs, which are subject to continuous stability measurements. The benefit of a fast batch release opposes the lower degree of characterization compared to higher-grade materials ⁵⁶
Reference material (RM)	A “material, homogeneous and stable with respect to one or more specified property values, which has been established to be for its intended use in a measurement process” ⁵³
Certified reference material (CRM)	A “material characterized by a metrologically valid procedure for one or more specified properties, accompanied by a reference material certificate that provides the value of the specified property, its associated uncertainty, and a statement of metrological traceability” ⁵³
NIST standard reference material® (SRM)	“A CRM issued by NIST that also meets additional NIST-specific certification criteria and is issued with a certificate or certificate of analysis that reports the results of its characterizations and provides information regarding the appropriate use(s) of the material” ⁵²



Table 2 Currently available materials for MNP research. This table is not comprehensive but should provide an overview. RGTM = research grade test material; RM = reference material; CRM = certified reference material; SRM = standard reference material. Abbreviations of the listed polymer types: PE = polyethylene; PET = polyethylene terephthalate; PMMA = poly(methyl methacrylate); PP = polypropylene; PS = polystyrene; PVC = polyvinyl chloride

Polymer type	Certified/property value (sizes = D_{50})	Grade	Supplier	Form	Intended use
PE (milled, aged)	61.2 μm	RM	BAM ⁷⁰	Dry powder, fragments	Instrument calibration
PET (milled)	62.6 μm	RM			
PS (milled)	206 μm	RM			
PS	Molecular weight, intrinsic viscosity, polydispersity	CRM		Pellet	
PS spheres	0.1 μm to 30 μm	SRM	NIST ⁷¹	Suspension	Instrument calibration
22 different types	400 μm –5 mm (up to 77 mm)	RGTM	Hawai'i Pacific University ⁷²	No additives stated Dry powder	Not specified/multi purpose
PP	1 μm	RGTM	CD Bioparticles ⁷³	Suspension	Not specified/multi purpose
PE	50 nm to 1 μm (and larger)	RGTM		Containing 0.1% Tween®20 + 2 mM	
PVC	250 nm and 400 nm	RGTM		NaN3 as biocide	
PS	40 nm to 1 mm	RGRM			
PMMA	25 nm to 1 μm	RGTM			

• Glycerol is commonly used to help disperse highly cohesive powders in aqueous liquids.^{77,78} Therefore, it promotes homogenous dilution into aqueous media, such as cell culture medium.

• It is well-tolerated at relatively high concentrations^{79,80} (up to 1.5 g kg⁻¹ oral and 1 g kg⁻¹ intravenous administration). Further administration routes for products containing glycerol include *e.g.*, buccal, intradermal, intravenous, dermal, nasal, inhalation, auricular, and ocular.^{81,82}

• In diluted form, glycerol is highly biocompatible in both cell-based assays⁸³ and *in vivo* models.⁷⁹

To test the hypothesis that PET and PP nanoplastic test materials stored in a glycerol medium fulfill the requirements outlined in the TPP, a comprehensive study was conducted to characterize their performance in a model *in vitro* cell culture assay system. Pristine, highly concentrated PET and PP nanosuspensions in glycerol (40 mg g⁻¹) were prepared and all pre-defined quality parameters characterized. The results indicate that the PET and PP nanoplastic research grade test materials are suitable for intended use in biological assays.

Materials and methods

Materials

Polypropylene (PP, CAS: 9003-07-0) and polyethylene terephthalate (PET, CAS: 25038-59-9) granules were kindly provided by PlasticsEurope. Tween®80 (polysorbate 80, P1754), glycerol ($\geq 99\%$, anhydrous for synthesis, 8.18709), xylene (IUPAC dimethylbenzene, isomeric mixture for analysis, 1.08297) and benzyl alcohol (IUPAC phenylmethanol, ReagentPlus®, 108006) were obtained from Sigma-Aldrich (Merck KGaA, Darmstadt, Germany). Filters were purchased from Whatman (0.8 μm , membrane filters, WHA7408004, Whatman plc, Maidstone, UK) and Merck Millipore (2 μm , PC membrane, TTP04700 and 0.45 μm , PVDF membrane,

SLHVR33RS, Merck Millipore KGaA, Billerica, USA). Ethanol (96%, v/v) was sourced from Brenntag (Brenntag Austria GmbH, Vienna, Austria). For vacuum filtration, a glass filter holder system was provided by VWR (511-0666, VWR International LLC., Radnor, USA). LB-agar and Sabouraud 4% glucose-agar were purchased from Carl Roth (X932.1, Carl Roth GmbH & Co. KG, Karlsruhe, Germany). Dulbecco's modified Eagle medium/nutrient mixture F-12 (DMEM/F-12, [L]-glutamine, no phenol red, 21041-025) was ordered from Thermo-Fisher (Fisher Scientific GmbH, Schwerte, Germany), whereas fetal bovine serum (FBS Superior, S0615) was obtained from Sigma-Aldrich (Merck KGaA, Darmstadt, Germany).

Preparation of nanoplastics

For the preparation of nanoplastics, methods from Achillas *et al.* (2009),⁸⁴ Lee *et al.* (2022),⁴⁶ and Tanaka *et al.* (2023)⁸⁵ were adapted and optimized (SOP available at DOI; <https://doi.org/10.5281/zenodo.14881493>). Briefly, PET (260 mg) was dissolved in benzyl alcohol (10 mL) while heated to 215 ± 0.2 °C in a silicone oil bath and stirred at 250 rpm for 45 min. The hot PET/benzyl alcohol solution (215 ± 0.2 °C) was transferred with a glass pipette into 15 min pre-cooled ethanol (125 mL, placed in an ice bath) while stirred at 400 rpm. The precipitated suspension was stirred for 3 min until cool and subsequently washed 5 times with ethanol (100 mL) by filtering. A polycarbonate membrane with a pore size of 2 μm was employed to retain nanoplastics, made possible by their rapid agglomeration during filtration. The particles on the filter were resuspended in fresh ethanol (26 mL) in a pre-weighed flask (m_{flask}) and subsequently sonicated in a temperature-controlled sonication bath (Sonocool SC 255, Bandelin electronic GmbH & Co. KG, Berlin, Germany) for 2 h at 21 ± 1 °C and 100% intensity. All sonication steps in this study were carried out with the same instrument and intensity (35 kHz, 180 W nominal power). Finally, the weight of the flask with suspension was determined (m_{susp}).



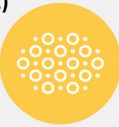






Nanoplastic test materials target product profile for the intended use in cell-based assays and <i>in vivo</i> toxicity tests	
1) 	Reproducible dispersibility in a range of aqueous media with physiological osmolarity
2) 	Free of additives, such as exogenous surfactants, which could confound test assay results
3) 	Free of process-derived contaminants, endotoxins, and micro-organisms
4) 	Stable in terms of size and sterility for at least one year, preferably at room temperature
5) 	Packaging that allows for dosing across a wide range of concentrations to enable dose-escalation studies
6) 	Reproducible in quantities realistic for distribution to multiple labs
7) 	Reproducible in terms of low batch-to-batch variation for key product characteristics

Fig. 1 Target product profile (TPP) of nanoplastic test materials for *in vitro* and *in vivo* use.

To prepare PP nanoplastics, the same procedure was performed with the following adaptations: PP granules (165 mg) were dissolved in xylene (80 mL) at 185 ± 0.2 °C. The hot solution (185 ± 0.2 °C) was added to ethanol (240 mL) as described above and the suspension was filtered through a $0.8 \mu\text{m}$ nylon membrane, undergoing the same rigorous washing protocol with ethanol to remove residual xylene. The washed material retained on the filter membrane was resuspended in ethanol (16 mL) and subsequently bath sonicated for 45 min at 21 ± 1 °C prior to weighing.

Concentration and product yield

Concentrations of nanoplastics in ethanol after washing were determined gravimetrically by transferring 0.5–1 mL suspension into a preweighed Eppendorf tube (2 mL, m_{empty})

and determining the fill weight (m_{filled}). The sample was then dried with a rotary evaporator (water bath at 50 °C, pressure 20 mbar, reduced incrementally) and the dry mass (m_{dry}) was determined. When the mass loss was $<1\%$, the concentration and percent yield were calculated with eqn (1) and (2):

Eqn (1): the concentration (c) of the washed nanosuspension calculated in mg g^{-1} .

$$c(\text{mg g}^{-1}) = \frac{(m_{\text{dry}} - m_{\text{empty}}) \times 1000}{(m_{\text{filled}} - m_{\text{empty}})} \quad (1)$$

Eqn (2): percentage yield

$$Y(\%) = \frac{c \times m_{\text{susp}}}{m_{\text{granules}}} \quad (2)$$

Transfer into glycerol

Glycerol stock suspensions (40 mg nanoplastics per g glycerol) was heated to 60 ± 1 °C and was mixed with the appropriate mass of ethanolic nanosuspension to achieve a final concentration of 40 mg nanoplastic per 1 g glycerol. The mixture was immediately vortexed and bath sonicated for 5 min to ensure even distribution. Ethanol was evaporated with a rotary evaporator at 50 °C by reducing the pressure in a stepwise manner to 20 mbar and the process was deemed completed when no more than 1% of mass loss was measured gravimetrically. Aliquots of the final suspension (1 g) were transferred into HPLC glass vials (1.5 mL), sealed and stored under exclusion of light in a cardboard box.

Determination of residual solvents

Samples of ethanolic nanoplastic suspensions (PET and PP) were drawn, vortexed and bath sonicated for 1 min before 1.8 mL were transferred into a 2 mL Eppendorf tube and centrifuged twice at $21380g$ for 2.5 min at room temperature. Subsequently, 1.5 mL of the supernatant was transferred into amber HPLC vials (2 mL) and analyzed with GC-MS (Trace1300/ISQ7000, Thermo Scientific Inc., Waltham, USA). Samples (1 μL) were injected directly and measured in triplicates. A CP-SIL-5 column (30 m, $0.25 \mu\text{m}$, 0.25 mm, Agilent Technologies Inc., Santa Clara, USA) was employed with Helium as the carrier gas. The solutions were run through the separation column using an autosampler in split mode (1:50) at an injection temperature of 260 °C. After the injection, the GC oven with the separation column was operated with the following temperature program: Temperature: 50 °C, Time: 15 min. At the end of the column, the gas flow from the separation column was transferred into the mass spectrometer at 250 °C. The MS spectra were recorded in the retention time range of 2 to 15 min, with the molecular fragments being detected in the range of 50 m/z (mass-to-charge ratio) to 200 m/z to exclude the solvent.

Contact angle measurements

To assess the surface hydrophobicity of the used materials, PET granules were melted onto a glass slide (200 °C, 5 min) and PP granules were cut with a scalpel to obtain flat



surfaces (reference starting material). A subset of the prepared PET and PP granules were heat treated for 128 h at 180 °C and 20 h at 140 °C, respectively (oxidized control). Ethanolic nanoplastics (intermediate product) were dried by vacuum filtration through a 0.8 µm nylon membrane. Dry nanoplastic powders and the prepared granules were fixed onto a slide with double-sided tape. Caution was taken to cover the whole surface with powder and compress it with a spatula before taking measurements. Compression was also necessary to prevent absorption of the water drop into the powder bed. Contact angles were measured with a drop shape analyzer (DSA30S, Krüss GmbH, Hamburg, Germany) using the sessile drop technique with de-ionized water as a test liquid. Individual measurements ($n = 30$) were taken for each sample, except heat treated (heat) PP ($n = 9$). The baseline was set manually and only measurements were included, where the software could correctly detect the droplet shape. Every measurement was performed at a new dry position. The droplet volume was set to 2 µL at a rate of 0.16 µL min⁻¹ and after a 5 s pause 6 measurements were taken with 1 frame per second. Individual measurement values are shown and the mean value calculated for statistical comparison.

Attenuated total reflection–Fourier transform infrared spectroscopy (ATR-FTIR)

Spectra were obtained with the Alpha II FTIR-spectrometer (Bruker Optics GmbH & Co. KG, Ettlingen, Germany) equipped with an ATR module (Platinum-ATR, single reflection ATR with a monolithic diamond). Before each measurement, blanks were recorded and automatically subtracted from the averaged spectrums. The dried nanoplastics and PET granules were transferred directly onto the ATR crystal, while PP granules were cut to obtain best contact with the ATR crystal. Five different batches of dried nanoplastics or starting material granules were tested with three technical replicates each consisting of 32 scans and an optical resolution of 4 cm⁻¹ between 4000 and 400 cm⁻¹. For processing (baseline correction and peak normalization) and analysis of the spectra, the SpectraGryph software (v1.2.16.1) was employed and averages are presented. To determine the carbonyl index (CI) of PP with eqn (3), the area of the peak of interest ($A_{C=O}$) from 1820–1650 cm⁻¹ was divided by the area of the reference peak ($A_{ref.}$) from 1500–1420 cm⁻¹.

Eqn (3): determination of the carbonyl-index (CI)

$$CI = \frac{A_{C=O}}{A_{ref.}} \quad (3)$$

Quality control (QC) dispersion protocol

For assessment of the particle size distribution characteristics of the test materials, a QC dispersion protocol was developed using the non-ionic, synthetic surfactant, Tween®80. The aim was to maximize particle deagglomeration to gain accurate

information on the primary particle size distribution characteristics of the product.

Dispersion from ethanol

When dispersing nanoplastics from the intermediate product (ethanolic suspension), 200 µL suspension were mixed with 800 µL of 5%, w/w Tween®80 in high purity water (HPW; step 1 dilution) followed by bath sonication at 21 ± 1 °C (15 min for PET and 40 min for PP, respectively). This suspension (typically 1 mg mL⁻¹ plastic content) was subsequently further diluted to the desired concentration in a 0.3% Tween®80/HPW (step 2 dilution), whereby the final Tween®80 content typically ranged from 0.35–0.39%.

Dispersion from glycerol

When dispersing nanoplastics from the glycerol suspension, the product was heated to 60 °C and vortexed vigorously to reduce the glycerol viscosity and ensure a homogenous suspension. A sample was then removed using a glass Pasteur pipette and 1 drop (~25 mg suspension containing ~1 mg nanoplastic) was added to a pre-weighed glass vial. The weight of the sample was determined and the mass of nanoplastics calculated. An appropriate volume of 5% w/w Tween®80 in HPW was added to the sample to achieve a nanoplastic concentration of 1 mg mL⁻¹ and bath sonicated at 21 ± 1 °C (15 min for PET and 40 min for PP, respectively). This suspension (step 1 dilution) was further diluted to the desired concentration in 0.3% Tween®80/HPW (step 2 dilution), whereby the final Tween®80 content typically ranged from 0.37–0.48%.

Biorelevant dispersion protocol

When performing cell culture studies, or investigations of the bio/ecocorona formed on the particle surface,^{86,87} it can be necessary to avoid the use of a synthetic surfactant as a dispersing agent. Therefore, a dispersion protocol using bovine serum albumin (BSA) and serum-supplemented cell culture medium as the dispersing agent was developed (SOP available at DOI; <https://doi.org/10.5281/zenodo.14881493>). Briefly, glycerol suspensions were heated, homogenized and one drop dispensed into a clean glass vial as described above. The PET sample (25 ± 0.25 mg) was mixed with 1000 µL of a 10% m/v aqueous BSA solution prepared in HPW (filtered through a 0.45 µm PVDF membrane, Millex®-HV, Low Protein Binding Durapore®) to achieve a nanoplastic concentration of 1 mg mL⁻¹ (step 1 dilution). The mixture was shaken gently to avoid air bubble formation and subsequently bath sonicated for 1 min at 21 ± 1 °C. Thereafter, distilled water or serum-supplemented cell culture medium was added (step 2 dilution) to achieve the final desired concentration and bath sonicated 15 min prior to further use. The more hydrophobic PP nanoplastics required a modified approach with 40 min of bath sonication at 21 ± 1 °C. The theoretical BSA concentration is typically 1.5% for a nanoplastic concentration of 150 µg mL⁻¹.



Scanning electron microscopy (SEM)

Samples of glycerol suspensions were washed by vacuum filtration and residues were resuspended in ethanol. These ethanolic suspensions were dropcast onto a glass slide, fixed onto a sample holder with double-sided conductive adhesive tape and dried overnight. On the following day, the samples were gold-sputtered and imaged with an EVO MA 10 (Zeiss, Oberkochen, Germany) using secondary electron contrast mode with voltages of 10 kV.

Particle size distribution and size stability after 12 months storage

The particle size distribution was measured using laser diffraction (LD) to detect the presence of agglomerates in the suspension. Dynamic light scattering (DLS) was also used to characterize batches where the majority of particles were in the submicron size range.

LD. Samples were dispersed either according to the QC or biorelevant dispersion protocols described above. After the step 1 dilution, QC samples were added stepwise into 6 mL 0.3% Tween®80 solution until an optical density value of 3–5% was achieved. The instrument (Mastersizer3000, Malvern Panalytical Ltd., Malvern, UK) performed 10 consecutive measurements and calculated the average particle size distribution. When using the biorelevant dispersion protocol, samples were added dropwise to 6 mL degassed cell culture medium (DMEM/F12 without phenol red) immediately after bath sonication until an optical density value of 3–5% was achieved (typically ~33 µg nanoplastics per mL) and the particle size distribution could be measured. Mie-Theory was applied using the following parameters for PET (RI: 1.636, absorption: 0.01) and PP (RI: 1.490, absorption: 0.01) at room temperature.

DLS. Samples were dispersed using the QC dispersion protocol and the step 1 diluted suspension was further diluted in distilled water to a concentration of 66 µg mL⁻¹. This was necessary to avoid turbidity and the measurement of Tween®80 micelles (Fig. S1†). These samples (700 µL) were then measured in a disposable PS cuvette (semi-micro, 67.742, Sarstedt AG & Co. KG, Nümbrecht, Germany) with Zetasizer Nano ZS (Malvern Panalytical Ltd., Malvern, UK). Measurements were conducted at 25 °C in backscatter mode (NIBS, 173°) and the “general purpose” analysis model using the same material properties as for laser diffraction and the built-in values for water as medium (RI: 1.330, Viscosity: 0.8872 cp).

Sterility

Sterility was tested using the pour-plate method,^{88,89} employing Lysogeny broth (LB) agar for evaluation of aerobic bacteria and Sabouraud 4% glucose agar for fungi detection. Nanoplastics in glycerol were dispersed using the biorelevant dispersion protocol to achieve final concentrations of 10, 50 and 200 µg mL⁻¹. Sterile glycerol mixed with cell culture media in the same amounts as used for the nanoplastic dispersion was used as a vehicle control. Dispersions (1000 µL) were then added to the agar plates and incubated for 3

days at 30 °C (LB plates) or 7 days at 20 °C (Sabouraud plates). The number of colony forming units (CFU) were counted and reported as CFU mL⁻¹. *Escherichia coli* and *Saccharomyces cerevisiae* were used as positive controls employing 10⁻⁹ and 10⁻⁵ serial dilutions, respectively.

Endotoxin content

Endotoxin content was assessed according to the STE-1.1 protocol issued by the Nanotechnology Characterization Laboratory using a limulus amebocyte lysate (LAL) assay (Pierce™ Chromogenic Endotoxin Quant Kit, Thermo Fisher Scientific Inc., Waltham, USA), including inhibition/enhancement controls with the same batches.⁹⁰ Briefly, samples were dispersed using the biorelevant dispersion protocol and diluted to a final concentration of 50 µg mL⁻¹ in Dulbeccos modified Eagle medium with fetal bovine serum (DMEM/F12+10% FBS). Each sample (50 µL) was transferred into a pre-equilibrated (37 °C) 96-well plate. Reconstituted amebocyte lysate (50 µL) was added and the mixture was incubated for 20 min. Subsequently, reconstituted chromogenic substrate solution (100 µL) was added and incubated for another 6 min. The reaction was stopped with acetic acid solution (25%, 50 µL). The absorbance was read at 405 nm using a UV/vis spectrophotometer (Epoch 2, Biotek Instruments Inc., Winooski, USA). Three technical replicates were measured per batch and the endotoxin level was calculated using standard curves ($R^2 > 0.980$). The mean limit of detection (LOD) and limit of quantification (LOQ) values for $n = 5$ calibration curves were 0.024 ± 0.009 EU mL⁻¹ and 0.073 ± 0.028 EU mL⁻¹ which corresponds to 0.002 ± 0.001 ng mL⁻¹ and 0.007 ± 0.003 ng mL⁻¹, respectively^{91,92} and are suitable for this study.

Osmolarity

DMEM and serial dilutions of DMEM+10% FBS+penicillin/streptomycin (DMEM_{compl.}) with glycerol were prepared in triplicate ranging from 6.2 to 0.05% (w/v) glycerol. The freezing point depression was measured using a K-7400S Semi-Micro Osmometer (Knauer Wissenschaftliche Geräte GmbH, Berlin, Germany) and the average osmolarity values (mOsmol) were calculated from $n = 3$ replicates.

Cytotoxicity

The human bronchial cell line, Calu-3 (ATCC-HTB-55, LGC Standards Ltd., Teddington, UK) was used for determining the cytotoxicity of glycerol and nanoplastic dilutions in media. A 3-[4,5-dimethylthiazol-2-yl]-2,5 diphenyl tetrazolium bromide (MTT) assay was employed with passage numbers 11–36 ($n = 11$ biological replicate experiments). Glycerol concentrations ranged from 0.04 to 20% (w/w) which equated to 0.05 to 25% (w/v) based on the density of glycerol at 60 °C (1.234 g cm^{-3})⁹³ as heating is required by the dispersion protocol. Nanoplastic concentrations of 10 to 150 µg mL⁻¹ were investigated. Cells were seeded at a density of 3×10^5 cells mL⁻¹ and incubated overnight. Cells were then incubated with the samples for 24 h (37 °C, 5% CO₂), after



which the MTT stock solution (20 μL , 5 mg mL^{-1}) was added. After 3.5 h, formazan crystals were dissolved in dimethyl sulfoxide (100 μL) and the absorbance was measured at 570 nm. As positive control (0% viability), cells were incubated with Triton®-X100 (0.25%), whereas untreated cells served as negative control (100% viability). The cell viability was calculated by using the following equation:

Eqn (4): Calculation of cell viability in%. $\text{OD}_{\text{sample}}$ = optical density of the treated cells; $\text{OD}_{\text{pos.ctrl}}$ = optical density of the positive control (0.25% Triton®-X100); $\text{OD}_{\text{neg.ctrl}}$ = optical density of untreated cells.

$$\text{CV (\%)} = \frac{\text{OD}_{\text{sample}} - \text{OD}_{\text{pos.ctrl}}}{\text{OD}_{\text{neg.ctrl}} - \text{OD}_{\text{pos.ctrl}}} \times 100 \quad (4)$$

Following guidance from the Nanotechnology Characterization Lab, the data is considered acceptable when the CV% was less than 50% for both control and sample replicates.⁹⁴ In our study, untreated cell controls exhibited a CV% of 12%, while CV% values of the treatment groups (when all test concentrations were pooled together) were 14%, 17% and 20% for nanoPET, nanoPP and glycerol samples, respectively. We therefore concluded that the data variability met standard acceptance criteria.

Data visualization and statistics

Raw data from laser diffraction (LD), dynamic light scattering (DLS) and ATR-FTIR measurements was exported with the respective software (Malvern's Mastersizer and Zetasizer software and SpectraGryph) and plotted with Python (v. 3.11.0) using the Matplotlib library (v. 3.6.3). Statistical tests were performed with Microsoft Excel (v. 1808, Built 10415.20025) and the Numpy library (v. 1.23.4) for Python.

Results and discussion

PET and PP nanoplastics: size, morphology and surface properties

The production of PET and PP nanoplastics was based on a combination of the methods reported by Achilias *et al.* (2009),⁸⁴ Lee *et al.* (2022),⁴⁶ and Tanaka *et al.* (2023).⁸⁵ These approaches used elevated temperatures to dissolve PET in benzyl alcohol (180 °C; 50 mg mL^{-1}) and PP in xylene (140 °C; 50 mg mL^{-1}) and injected the hot solutions into *n*-hexane (60 mL), methanol (60 mL), ethanol (100 mL) or DMSO (100 mL) at room temperature under stirring conditions. The solvents (benzyl alcohol and xylene) were subsequently removed by rinsing the nanospensions with acetone or hexane using a 0.2 μm PTFE or polyester filter. In order to avoid complications with high concentrations of DMSO, we chose to precipitate the PET and PP into ethanol as an anti-solvent and rinsing agent. In a final step, we used rotary evaporation to exchange ethanol with glycerol, a non-volatile, biocompatible storage medium with preservative properties (Fig. 2A and B).⁷⁶

Nanomaterials produced in this manner were roughly spherical (Fig. 2C and D) with similar primary particle diameters between the two polymer types. QC measurements of the ethanolic intermediate product revealed reproducible size distributions where >90% of the particles were below the desired 1 μm threshold (Fig. S2, Table S1†). Product yields for a typical batch size of 255 ± 5 mg and 165 ± 3 mg were $90.6 \pm 3.3\%$ and $91.2 \pm 1.5\%$ for PET and PP nanoplastics, respectively (Tables S2 and S3†). Thus, 230 mg of PET and 150 mg of PP nanoplastics can be produced with this method per day. Residual solvents (in particular benzyl alcohol and xylene) were quantified for a single batch of PET (#118) and PP (#077) nanoplastics using GC-MS. Benzyl alcohol was not detected in either sample. Unquantifiable traces of xylene were only found in the PP sample.

The surface hydrophobicity was investigated with contact angle measurements and revealed larger contact angles (thus higher hydrophobicity) for PP compared to PET, which is expected based on the polymer structures (Fig. 3A). Heat treatment (heatPET: 128 h at 180 °C; heatPP: 20 h at 140 °C) was used to induce surface oxidation and act as a positive control resulting in smaller contact angles as expected. Surprisingly, both nanoplastics (nanoPET/PP) showed significantly higher contact angles compared to the starting materials (nativePET/PP, native polymer granules), indicating an increase in surface hydrophobicity. This observation is likely an effect of the nanostructured topography of the compacted nanoplastic samples,⁹⁵ commonly referred to as the lotus effect, which is known to increase surface hydrophobicity and water repellency.⁹⁶

ATR-FTIR was used to characterize the chemical composition of the nanomaterials. Bulk information on the entire particle is obtained since the penetration depth of ATR-FTIR is generally larger than the primary diameter. The PET/PP nanomaterials are compared to the starting materials as well as the native materials after heat treatment. Heat treatment did not affect both polymer types equally. Except for a slight colour change, PET did not show any other visual signs of degradation. PP turned intensively yellow and showed surface cracks, hence oxygen was able to penetrate deeper layers of the material. As reported in literature, the IR spectrum of heat treated PET (heatPET, Fig. 3B) shows a broadening between 550–650 cm^{-1} of the peak at 720 cm^{-1} compared to the starting material (nativePET), which is attributable to aromatic C–H out of plane bending.⁹⁷ The spectrum of PET nanoplastic (nanoPET) mostly overlaps with nativePET and does not show the additional peaks of heatPET. Therefore, a chemical change due to the production process can be excluded. However, nanoPET shows an additional OH stretching vibration at 3200–3500 cm^{-1} which is likely a sign of residual solvent that could not be fully removed. It is hypothesized that the higher polarity of PET favors polar interaction with ethanol and hinders its complete evaporation, which may account for the absence of this band in the PP nanoplastic (nanoPP) spectrum. Another possibility is that this band originates from residual benzyl



A) Protocol for nanoPET B) Protocol for nanoPP

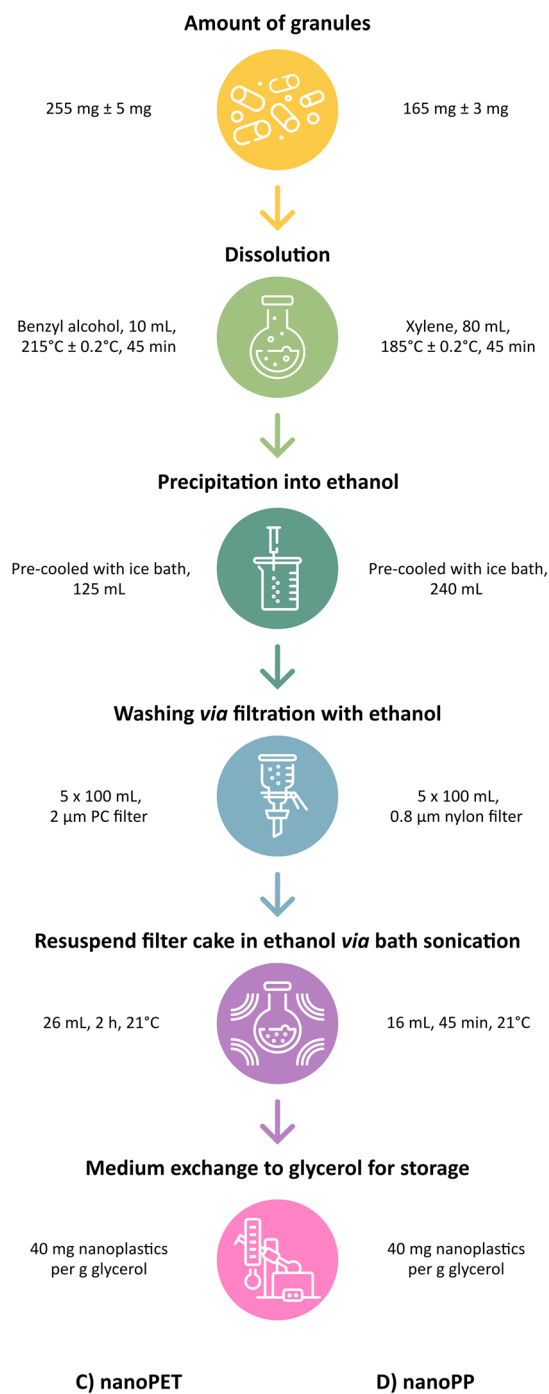


Fig. 2 Production scheme of PET (A) and PP (B) nanoplastic suspensions. Overview of controlled parameters and the experimental settings used. Representative SEM micrographs of PET (C) and PP (D) nanoplastics.

alcohol, which shows features in this area, although other stronger benzyl alcohol peaks are missing in the nanoPET spectrum.

The heat treated PP (heatPP, Fig. 3C) shows a pronounced carbonyl peak at 1650 cm^{-1} , smaller signals at 1550 cm^{-1} and 1750 cm^{-1} , and a broad absorption band between 3100–3650 cm^{-1} corresponding to formed hydroxyl bonds.⁹⁸ The overlay of the starting material (nativePP) and the PP nanoplastic (nanoPP) spectra did not show relevant differences, especially in the carbonyl region where heatPP did exhibit additional signals. It was therefore concluded, that the production process did not alter the chemical profile of the PP and no residual solvents remained in the nanoPP. Additionally, the carbonyl index (CI) value can be calculated for aliphatic polymers like PP using eqn (3) and provides information about the oxidation status of the material. The CI of nanoPP was similar to the nativePP but significantly lower than heatPP (Fig. 3D). ATR-FTIR spectra of five batches of both PET and PP nanoplastics also revealed a very low batch-to-batch variability (Fig. S3 and S4†).

Particle size distribution: quality control

The high surface hydrophobicity of the relatively pristine PET and PP nanoplastics makes dispersion into aqueous media challenging. Pilot experiments indicated that high surfactant concentrations, high energy inputs *via* bath sonication, and long sonication times were required to reliably deagglomerate as much of the nanosuspension as possible to reflect the primary particle size distribution. An optimized QC dispersion protocol using a relatively high content of the non-ionic surfactant Tween®80 was developed specifically for determination of the particle size distribution characteristics of the materials (Fig. 4A and B).

Although DLS is considered the more appropriate method for determination of submicron sized materials, this technique presented three major challenges for QC size measurements of the nanoplastics: 1) DLS does not cope well with the presence of micron-sized agglomerates in the system, 2) it has difficulties with very low or high density materials, which exhibit flotation or sedimentation during the relatively short DLS measurement times and 3) the final concentration of Tween®80 used in our QC dispersion standard operating procedure (SOP) is above the critical micelle concentration (0.0014%, m/v),⁹⁹ resulting in the detection of Tween®80 micelles in the 10 nm range which has been reported previously (Fig. S1†).^{99,100} We therefore explored LD as a complementary technique for QC size measurements, which was not as sensitive to these issues. In fact, we found that the LD-generated particle size distribution curves were more informative for QC studies of the nanoplastics under a variety of conditions. Comparisons of DLS and LD measurements on the same batch of materials also show roughly similar values, demonstrating that size distribution profiles generated by LD can provide a fairly accurate depiction of the material size characteristics,



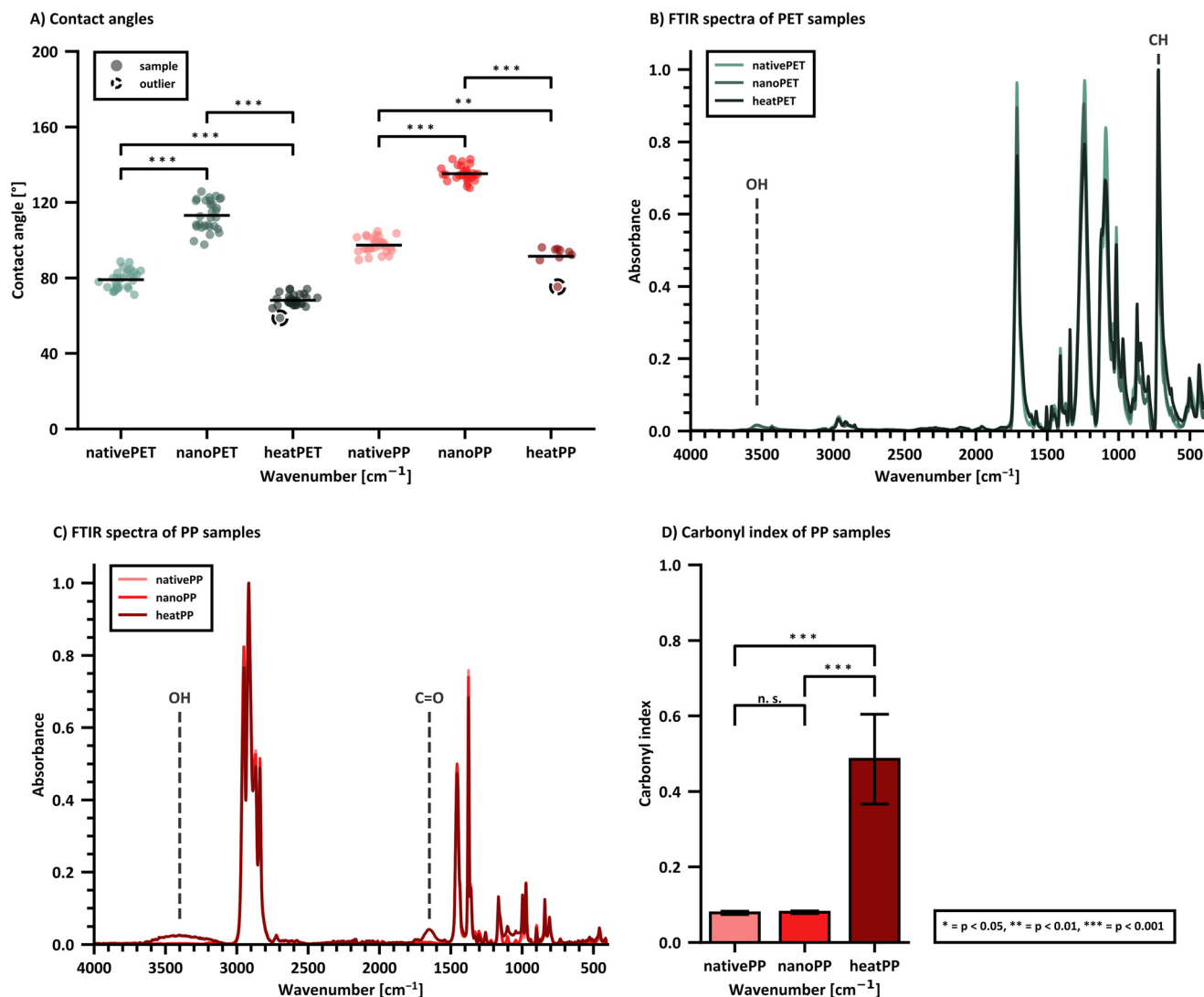


Fig. 3 Surface hydrophobicity and bulk chemical composition of dried PET and PP nanoplastics (prepared from the intermediate ethanolic suspension) compared to the respective starting material was assessed via contact angle measurements (A) and ATR-FTIR spectra (B and C). The respective carbonyl index value of PP (D) was calculated from its ATR-FTIR spectrum. Contact angle measurements (30 droplets per material except heatPET with 9 droplets) were collected for one representative nanomaterial batch (PET: batch 118, PP: batch 077), while ATR-FTIR spectra were collected from five batches of nanoPET and nanoPP (measured in three technical replicates). Statistical significance was tested with a one-way ANOVA, where * $p < 0.05$, ** $p < 0.01$, and *** $p < 0.001$.

dispersibility and batch-to-batch variability (Fig. 4C–H). It should be noted, that the sizes generated by the respective scattering techniques are calculated hydrodynamic diameters of hypothetical spheres with the equivalent volume as the measured particle and are therefore less accurate for irregularly shaped particles.¹⁰¹ This explains the differences between the observed diameters on SEM images and the hydrodynamic diameters.

Batch-to-batch variability was evaluated using key particle size descriptors derived from LD measurements (Table 3). From the overlaid size distribution curves in Fig. 4G and H it can be seen that each batch contains a small fraction of larger agglomerates in the micron size range, which cannot be fully dispersed despite the aggressive conditions of the QC dispersion procedure. During SEM imaging, no primary

particles above 1 μm were detected. Although more images would be necessary for representative size analysis, only agglomerates were larger than 1 μm . Further, multiple measurements showed a higher variability of the D_{90} values (90% of the particle population has a particle size smaller than this diameter), but has less of an impact on the median particle size (D_{50}). Interestingly, the most stable and informative particle size distribution descriptor is the percentage of particles in the submicron size range (% <1 μm).

It is worthwhile to mention that early batches (#100–107) of the PET nanoplastics showed a higher prevalence of non-dispersible agglomerates. Investigations revealed that a slightly higher solution temperature (215 °C) and tight control over temperature variations during the precipitation



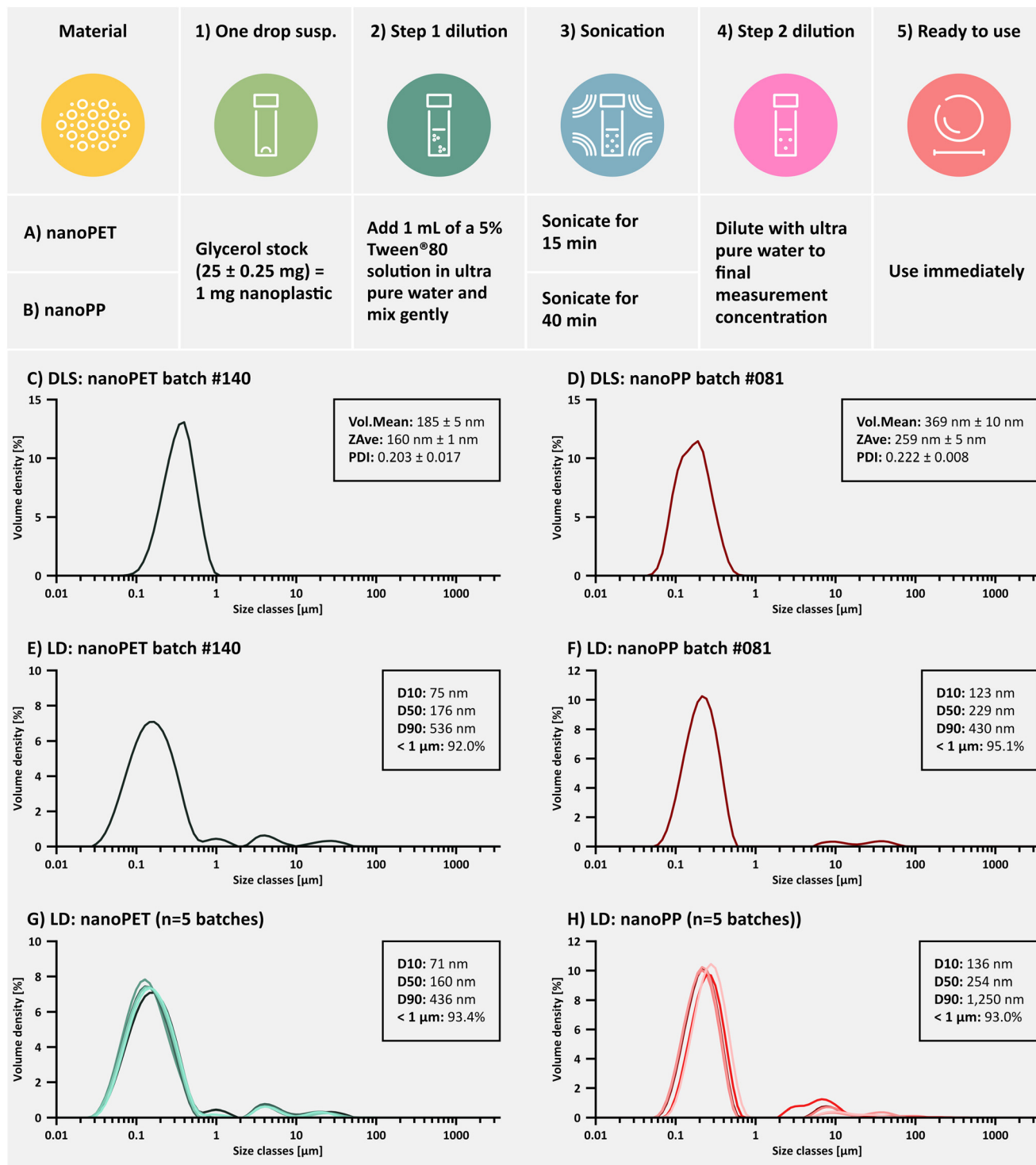


Fig. 4 Dispersion protocols used for the quality control of PET (A) and PP (B) nanoplasic samples. Comparison of DLS and LD particle size distribution curves for matched PET (C and E; batch 140) and PP (D and F; batch 081) nanoplasic samples dispersed from glycerol using the QC dispersion protocol. Common size descriptors from each measurement technique are provided in the insets. Batch-to-batch reproducibility of the particle size distribution is shown $n = 5$ independent batches of PET (G) and PP (H).

process (± 0.2 °C) effectively increased the % of particles < 1 μ m from $69 \pm 6\%$ (9% RSD) to $92 \pm 1\%$ (1% RSD) once a stricter temperature control was implemented. It was of further relevance to note that differences in size distribution profiles between the ethanolic suspension (intermediate

product) and the glycerol suspension (final product) were minimal (Fig. S5 and S6†). Additionally, stability studies were performed for samples stored in glycerol over 12 months. The D_{10} (10% of the particle population has a particle size smaller than this diameter) and D_{50} (median) values varied



Table 3 Size uniformity of PET and PP nanoplastic glycerol batches following dispersion using the biorelevant dispersion protocol ($n = 3$ separate dispersion events from a single batch). Particle size distribution descriptors were derived from LD measurements. D_{10} : 10% of the particle population has a particle size smaller than this diameter, D_{50} : median, D_{90} : 90% of the particle population has a particle size smaller than this diameter. Values depict the mean \pm standard deviation values with the relative standard deviation (%) provided in parentheses. Please note, diameters are reported in μm

System	Dispersion SOP	$D_{10} \pm \text{SD}$ [μm] (RSD%)	$D_{50} \pm \text{SD}$ [μm] (RSD%)	$D_{90} \pm \text{SD}$ [μm] (RSD%)	% $< 1 \mu\text{m} \pm \text{SD}$ (RSD%)
PET	Biorelevant ($n = 3$ dispersions from batch #121)	0.101 ± 0.005 (5.1%)	0.236 ± 0.012 (5.2%)	3.33 ± 0.45 (13.4%)	86.5 ± 1.7 (1.9%)
PP	Biorelevant ($n = 3$ dispersions from batch #081)	0.241 ± 0.005 (1.9%)	0.528 ± 0.004 (0.7%)	4.64 ± 1.93 (41.7%)	74.5 ± 1.3 (1.8%)

$< 15\%$ (RSD) and % $< 1 \mu\text{m}$ remained above 85%, thus meeting the specifications set by the TPP (Fig. S7, Table S4†).

Particle size distribution: dispersibility in biorelevant media

To assess the particle size distribution under conditions suitable for cell culture studies or indeed when studying the formation of an eco-corona on the nanoplastic surface,^{86,87} a dispersion protocol in biorelevant media is necessary. In the current study, we devised an exemplary biorelevant dispersion protocol suitable for cell culture studies using the

protein, bovine serum albumin, as a primary dispersing agent. In this particular SOP, a two-step dispersion procedure was employed, in which the nanoPET or nanoPP test materials in glycerol were first dispersed in concentrated BSA (10%), followed by a second dilution (step 2 dilution) into complete cell culture medium (cDMEM = DMEM supplemented with 10% FBS and 1% penicillin/streptomycin) (Fig. 5A and B).

It was hypothesized that such a biorelevant dispersion protocol might not be as effective in preventing nanoplastic agglomeration compared to high concentrations of the

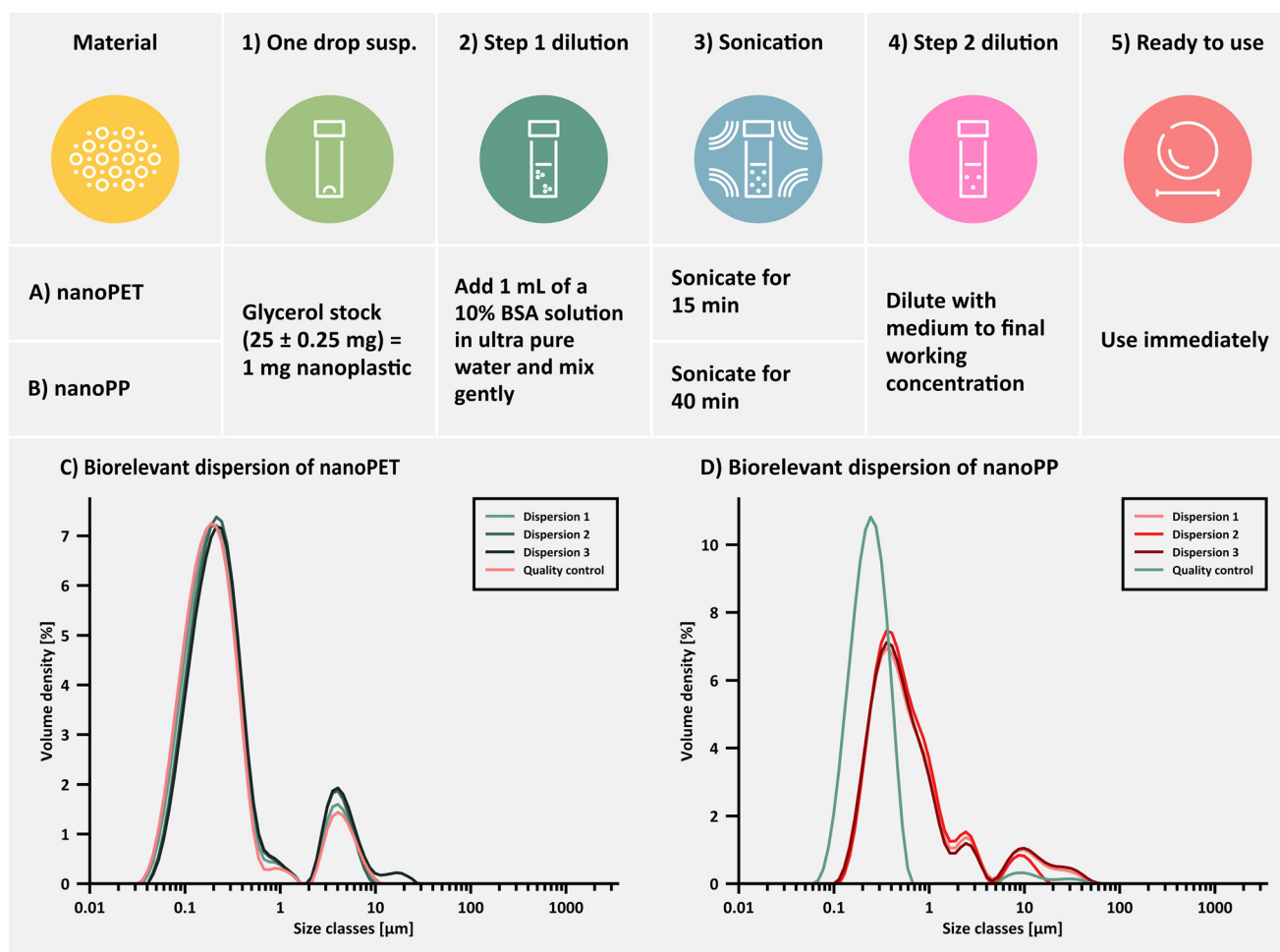


Fig. 5 LD particle size distribution curves for PET (C; batch #121) and PP (D; batch #081) nanoplastic samples dispersed from glycerol using the biorelevant dispersion protocol (A for PET, B for PP; $n = 3$ dispersion events). The light red (PET) and light blue (PP) traces show the same batch of nanoplastics dispersed using the quality control protocol for comparison.



synthetic surfactant, Tween®80 (QC dispersion). Fortunately, the more hydrophilic PET nanoplastics could be fully dispersed using the biorelevant dispersion protocol showing no relevant differences to the QC dispersion protocol (Fig. 5C) when applied to the same batch. In contrast, the more hydrophobic PP nanoplastics showed a reproducible shift towards larger particle sizes using the biorelevant dispersion protocol (Fig. 5D). % <1 µm was slightly lower than the average dispersion using the QC protocol in both cases (Table 3). Studies on the binding capacity and affinity of proteins (specifically BSA) to the PP and PET nanoplastic surface are scarce. We hypothesize, that the difference in re-dispersibility between PET and PP in biologically relevant medium is mainly driven by the different surface hydrophobicity characteristics and therefore protein coverage, but more focussed studies with a head-to-head comparison are needed (please refer to the ESI for further literature references to protein binding studies). A range of different biorelevant proteins and ecologically relevant surfactants^{50,87} are currently under investigation for their ability to homogeneously disperse the PET and PP nanoplastics studied here (unpublished data) but preliminary results indicate that each dispersing agent behaves differently, therefore requiring the development of bespoke dispersion protocols for every new system.

Sterility and endotoxin content

Due to the usage of volatile solvents and elevated temperatures, it was not possible to produce PET and PP nanoplastics under fully aseptic conditions. However, the utilization of organic solvents in clean fume hoods combined with minimal handling steps should theoretically minimize accidental contamination with viable microorganisms as well as fungal spores from the ambient lab environment. Sterility testing of 22 batches of PET and PP nanoplastics was performed with materials diluted to 10, 50 and 200 µg mL⁻¹ using the biorelevant dispersion protocol. None of the batches tested showed evidence of microbial contamination (0 CFU mL⁻¹). Positive controls with *Escherichia coli* (641 ± 187 CFU mL⁻¹) and *Saccharomyces cerevisiae* (452 ± 51 CFU mL⁻¹) were performed to verify assay functionality. Negative controls with glycerol diluted in cell culture medium and sterile water (0 CFU mL⁻¹) were also carried out. Additionally, an unopened vial of the PET batch #025 and PP batch #026 was tested after 10 and 12 months storage at ambient room temperature. Neither sample showed any indication of microbial growth.

Endotoxin content of cell culture medium controls and nanoplastics diluted to 50 µg mL⁻¹ using the biorelevant dispersion protocol (*n* = 13 batches) did not reveal any values above the LOD (0.024 ± 0.009 EU mL⁻¹). Thus, we conclude that the respective nanoplastic preparation methods did not result in measurable endotoxin contamination. The results demonstrate that the material also does not exceed the suggested maximal contamination value of 0.1 EU mL⁻¹

recommended by Li *et al.* for *in vitro* experiments.^{102–104} It must be noted that non-endotoxin pyrogens or other bacterial/fungal or viral contaminants can also influence *in vitro* and *in vivo* tests.¹⁰⁵ The Ph. Eu. 11 (chapter 5.1.10) approves the monocyte activation test to assess for non-endotoxin pyrogens and should be employed in future studies, especially when larger batches are produced.

Osmolarity and cytotoxicity

When diluted directly into cell culture medium, residual glycerol can contribute to an increase in osmolarity (Table 4). The osmolarity of the test system is important for cytotoxicity studies, since both hypo- and hypertonic samples can stress cells causing artefactual cellular responses,^{106–109} which could be mistakenly attributed to the test material. Many cell types can tolerate deviations from physiological osmolarity from approximately 290–390 mosmol, although certain cell types can be more sensitive than others.^{110,111} Therefore, testing of vehicle controls (including glycerol in this case) is always recommended. Table 4 provides an overview of the respective amounts of glycerol and nanoplastics present in a series of dilutions prepared with the biorelevant dispersion protocol. The corresponding osmolarity values from three replicate measurements are provided showing that dilutions exceeding 0.8% (w/v) glycerol exhibit hyperosmotic characteristics, *i.e.* an osmolarity >400 mOsmol.

To characterize the effects of the PET and PP nanoplastic test materials (and their possible content on residual components) on cell viability, *in vitro* cytotoxicity experiments were performed. First, the effects of pure glycerol added to cell culture medium in concentrations ranging from 0.05–25% w/v were assessed (Fig. 6A) followed by experiments evaluating the effects of nanoplastics diluted in cell culture medium (nominal particle concentration: 10–150 µg mL⁻¹; Fig. 6B and C) which corresponds to a glycerol concentration of 0.025–0.38% (w/v). The MTT assay, which measures the metabolic activity of cells, was performed using a human bronchial cell line (Calu-3). Cells were incubated with the test systems for 24 h and the cell viability compared to the untreated control group was determined. When comparing the cytotoxicity results of the nanoPET (density: 1.38 g cm⁻³)¹¹² with the nanoPP (density: 0.90 g cm⁻³ according to the data sheet) data, it should be noted that a higher concentration of the nanoPET is expected to reach the Calu-3 cell layer *via* sedimentation and diffusion processes^{113–115} compared to the low-density nanoPP, which will be prone to flotation. At the highest concentration of nanoPP tested, the cell viability appeared to decrease but not significantly. Ongoing studies using an expanded concentration range are underway to determine whether this is a real sample-induced effect, an effect of the vehicle, which might include residual production components or a particle-induced effect.

The optimal osmolarity for Calu-3 cells ranges from 290–390 m Osmol. This corresponds well with our observations that glycerol is well-tolerated up to 0.8% (w/v) (394 ± 2



Table 4 Mean osmolality values of different amounts of glycerol (% w/v) added to DMEM + 10% FBS. Values represent the mean and standard deviation of $n = 3$ experiments

Vehicle	Amount glycerol (% w/v) added	Nanoplastic concentration ($\mu\text{g mL}^{-1}$) in dilution ^a	Osmolality (mOsmol)
DMEM + 10% FBS	0	—	314 \pm 2
	0	—	319 \pm 3
	0.05	20	323 \pm 1
	0.1	40	326 \pm 1
	0.2	80	336 \pm 2
	0.4	160	351 \pm 12
	0.8	320	394 \pm 2
	1.6	640	485 \pm 4
	3.1	1240	656 \pm 4
	6.2	2480	1009 \pm 12

^a Nanoplastic concentrations in each dilution are calculated based on application of the biorelevant dispersion protocol for a nanoplastic sample in glycerol (40 mg plastic per g glycerol).

mOsmol) over a 24 h period (Fig. 6A). At higher glycerol concentrations, the cell viability drops below the 70% cytotoxicity threshold defined by ISO 10993.¹¹⁶ Shorter incubation times will enable the use of a higher glycerol content. For example, R. Scherließ reported that Calu-3 cells exposed to increasing concentrations of glycerol for only 4 h exhibited a half-maximal cytotoxic concentration (CC_{50}) of 2.8 mol L^{-1} ($3457 \pm 12 \text{ mOsmol}$), *i.e.* nearly 10-fold higher than the CC_{50} value determined for a 24 h incubation.⁸³ The tested plastic concentration range corresponds to the most commonly used concentration range for *in vitro* cytotoxicity experiments in this field of study^{117–119} supporting the conclusion that the amount of glycerol used as a storage medium should not negatively impact cytotoxicity studies up to these nanoplastic concentrations. However, further studies with a wider range of cell types, including different cell lines and primary cells, are underway to determine the wider applicability of this conclusion. It is also important to highlight that the impact of glycerol on the function of a wider range of biological assays should be assessed.

Outlook

To our knowledge, there are currently no nanoplastic reference materials certified specifically for use in *in vitro* and *in vivo* biological assays. Therefore, there are also no precedences for the development of this type of reference material. On the other hand, the research community has reported an urgent need for well-defined nanoplastics for an intended use in biological and toxicology studies,^{45,47–51} thus there is a strong rationale for exploring the boundaries of reference material development. Based on the more complex requirements for intended uses in biological systems, such as colloidal stability in complex aqueous media, sterility and low endotoxin content, it may be necessary to expand the certification criteria and include further critical quality attributes (CQA). Table 5 lists the CQA which we propose and the acceptable specification limits for each attribute.

With the current approach, five out of six requirements of the proposed TPP could be fulfilled for both nanomaterials. It was notable that dispersion of the nanoPP in biorelevant media could not achieve the original particle size distribution requiring further development work. Also, the content homogeneity of a higher number of vials needs to be investigated. Further aspects which require additional investigation include storage stability over longer time periods and in-use shelf-life. Glycerol is known to be hygroscopic when used in high concentrations.⁷⁶ Although no noticeable change in particle size distribution, microbial growth or endotoxin content was observed within 12 months in unopened containers, we have not yet extensively investigated these parameters under in-use conditions, *i.e.* multiple openings of the vials. Particle shape is another important property that needs to be considered in future work to resemble the environmental situation. It has also been shown that shape can affect colloidal stability¹²¹ of NPs and their uptake.¹²²

One of the reasons that content homogeneity studies were not performed in the current work was the small number of vials produced with the lab scale production method. Scale-up from tens to hundreds of milligrams was possible without much optimization effort when ratios were kept constant. However, scale-up to even larger batch quantities is difficult without switching from manual towards automated methods. For example, if a temperature controlled automated pump system could be employed for the precipitation step, yields up to gram amounts per batch are feasible and even a continuous precipitation process could be developed. After large-scale production, homogeneity needs to be demonstrated before gaining reference material status. Independent confirmation of CQAs such as particle size distribution, sterility and endotoxin content should also be performed *via* an inter-lab comparison study. Finally, a broad discussion including international organizations, policy makers and the research community is needed to refine the proposed TPP and provide guidelines for reference materials producers of nanoplastics for intended use in biological assays.



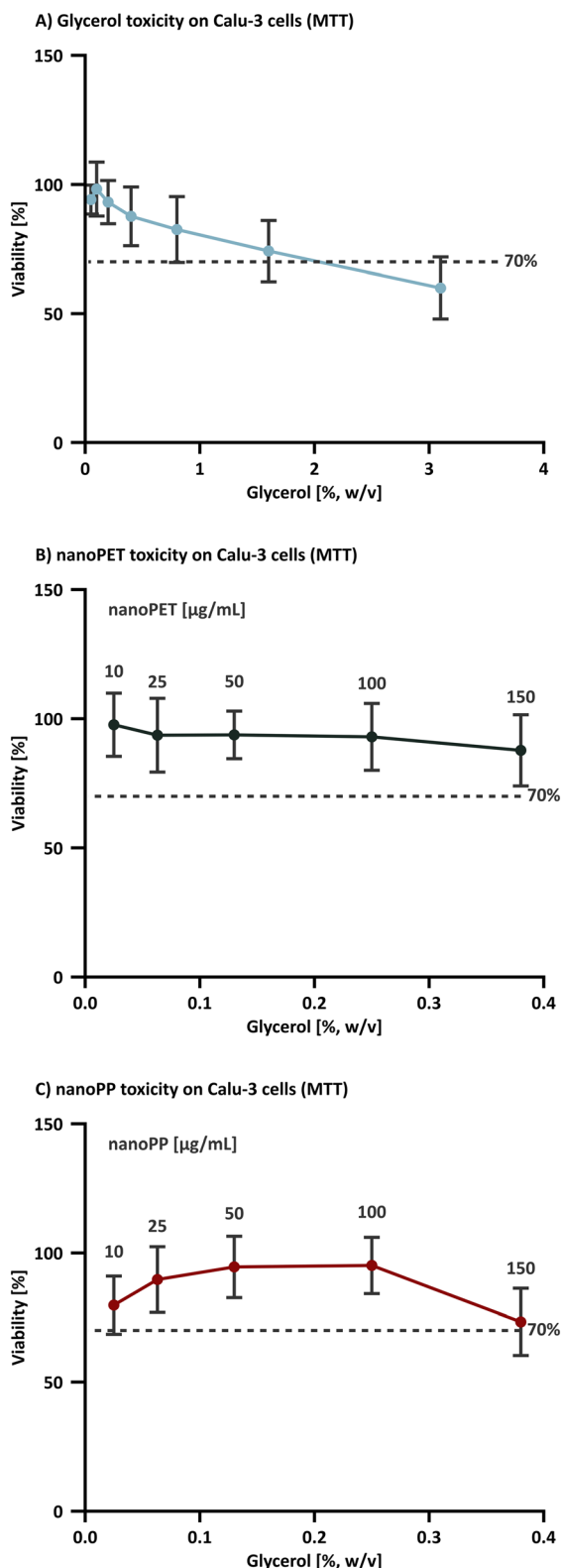


Fig. 6 Viability of Calu-3 cells after 24 h exposure to different test systems: (A) glycerol in concentrations of 0.05; 0.1; 0.2; 0.4; 0.8; 1.6; 3.1% (w/v). Values presented are the mean and standard deviation from $n = 11$ replicate experiments with different cell passage numbers. The viability of Calu-3 cells incubated 24 h with PET (B) and PP (C) nanoplastics diluted to 10–150 $\mu\text{g mL}^{-1}$ (containing 0.025; 0.063; 0.13; 0.25; 0.38% (w/v) glycerol). Values presented are from $n = 5$ replicate experiments with different cell passage numbers.

Conclusions

Using a QbD-inspired approach to product development, PET and PP nanoplastic research grade test materials were developed in this study for intended use in biological assays. Encouragingly, the data generated here indicates that these prototype nanoplastics are suitable in terms of particle size distribution, uniform dispersibility, size stability over 12 months storage, sterility, low endotoxin content and biocompatibility for their intended use. Compared to other published test systems, critical material attributes for biological assays were considered (sterility, endotoxins, solvent residues), material and study comparability were assured (batch-to-batch variability, storage stability) and practicality through transparent reporting of production time and yield has been shown. Further studies are recommended to assess long-term stability complying with the ISO 33405:2024 standard⁵⁴ and whether the glycerol storage medium does not interfere with a wider panel of commonly used biological assays at concentrations present following dilution. In the course of this investigation, the importance of optimized, bespoke dispersion protocols for nanoplastics in biorelevant media became increasingly evident. For potential users of these test materials this would mean that the responsibility of optimizing and validating biorelevant dispersion protocols for different dispersion media would fall to individual laboratories. With the help of a validated QC dispersion protocol and an example of a bespoke biorelevant dispersion protocol, we have provided a workflow which users can adopt to assess the impact of their own dispersion process on the nanoplastic size distribution profile, which is one of the most important variables tested in studies on particle toxicity. In conclusion, research grade test materials comprised of PET and PP nanoplastics were developed with promising perspectives to achieve wider spread use in biological assays examining the impact of nanoplastics on human health.

Data availability

Data for this article, including standard operating procedures, spreadsheets of all measurements, particle size distribution data and FTIR spectra have been published in Zenodo: DOI: <https://doi.org/10.5281/zenodo.14881493>. A part of the data supporting this article have also been included as part of the ESI.†

Author contributions

L. Wimmer: conceptualization, investigation, methodology, data curation, writing – original draft; MV Nguyen Hoang: investigation, writing – review and editing; J. Schwarzing: investigation, writing – review and editing; V. Jovanovic: investigation, writing – review and editing; B. Andelković: investigation, writing – review and editing; T. Cirkovic Velickovic: conceptualization, funding acquisition, writing – review and editing; T. C. Meisel: conceptualization,



Table 5 Proposed list of CQA (i.e. properties of interest) and their corresponding specifications recommended for reference nanoplastics intended for use in biological assays

CQA	Specification	Recommended methods/comments
Homogeneity of particle concentration (uniformity of nanoplastic content across several units)	Guidelines do not provide a recommendation for a maximal allowable variability. We suggest 85–115% of the target value ¹²⁰	For batches with >100 units, a minimum of 10 units measured in duplicates. For batches with <100 units, at least 3 units or 10% of the batch size measured with four technical replicates ⁵⁴
Homogeneity of the particle size distribution profile	>85% of the particles are <1 µm using the validated QC dispersion protocol	Particle size distribution data should be determined using a validated QC dispersion protocol combined with LD analysis
Stability of the particle size distribution profile	D_{10} and D_{50} measured after 12 months storage at ambient room temperature should not differ >15% from the original values. The % <1 µm should not drop below 85%	Particle size distribution data should be determined using a validated QC dispersion protocol combined with LD analysis
Sterility after manufacture and storage	0 CFU mL ⁻¹ after production and 12 months storage of unopened containers at ambient room temperature	Sterility should be tested using a validated method following dispersion using a validated biorelevant dispersion protocol with sterile cell culture media
Endotoxin content measured after manufacture	<0.1 EU mL ⁻¹ (ref. 92)	Endotoxin content should be tested using a validated method following dispersion using a validated biorelevant dispersion protocol with sterile, low-endotoxin grade cell culture media
Residual solvents from the production process	Residual solvents <1%	GC-MS. If no biological effect is expected, higher amounts of residuals could be acceptable

methodology, writing – review and editing; Tassilo Waniek: investigation, methodology, writing – review and editing; Christiane Weimann: investigation, writing – review and editing; Korinna Altmann: conceptualization, funding acquisition, methodology, writing – review and editing; Lea Ann Dailey: conceptualization, funding acquisition, methodology, supervision, writing – review and editing.

Conflicts of interest

The authors declare no conflicts of interest.

Acknowledgements

This work was supported by funding from the EU's H2020 framework program for research and innovation under grant agreement no. 965173 (Imptox), no. 964766 (POLYRISK) and no. 965367 (PlasticsFate). All three projects are part of the European cluster to understand the health impacts of micro- and nanoplastics (CUSP). The authors would like to warmly thank Ing. Claudia Mitterer for granting access to the drop shape analyser and Dr. Itziar Otazo Aseguinolaza for initial method testing. Furthermore, the authors thank Dr. Gisbert Rieß (Montanuniversität Leoben) for providing the GC-MS measurement results and Dr. Friedrich Menges for providing a free license of SpectraGryph.

References

- 1 B. C. T. de Deus, T. C. Costa, L. N. Altomari, E. M. Brovini, P. S. D. de Brito and S. J. Cardoso, Coastal plastic pollution: A global perspective, *Mar. Pollut. Bull.*, 2024, **203**, 116478.
- 2 European Commission, *Commission Staff Working Document - A European Strategy for Plastics in a Circular Economy*, Brussels, 2018.
- 3 5/14 United Nations Environment Assembly, End Plastic Pollution: Towards an International Legally Binding Instrument - Resolution adopted by the United Nations Environment Assembly on 2 March 2022 [UNEP/EA.5/Res.14], 2022.
- 4 The White House, FACT SHEET: Biden-Harris Administration Releases New Strategy to Tackle Plastic Pollution, Takes Action to Reduce Single-Use Plastics in Federal Operations, FACT SHEET: Biden-Harris Administration Releases New Strategy to Tackle Plastic Pollution, Takes Action to Reduce Single-Use Plastics in Federal Operations, https://www.whitehouse.gov/briefing-room/statements-releases/2024/07/19/fact-sheet-biden-harris-administration-releases-new-strategy-to-tackle-plastic-pollution-takes-action-to-reduce-single-use-plastics-in-federal-operations/?utm_source=link, (accessed 30 August 2024).
- 5 J. Soares, I. Miguel, C. Venâncio, I. Lopes and M. Oliveira, Public views on plastic pollution: Knowledge, perceived impacts, and pro-environmental behaviours, *J. Hazard. Mater.*, 2021, **412**, 125227.
- 6 Plastics Europe, *Plastics - the fast Facts 2023*, 2023.
- 7 N. Singh and T. R. Walker, Plastic recycling: A panacea or environmental pollution problem, *npj Mater. Sustain.*, 2024, **2**, 17.
- 8 W. W. Y. Lau, Y. Shiran, R. M. Bailey, E. Cook, M. R. Stuchtey, J. Koskella, C. A. Velis, L. Godfrey, J. Boucher, M. B. Murphy, R. C. Thompson, E. Jankowska, A. C.



- Castillo, T. D. Pilditch, B. Dixon, L. Koerselman, E. Kosior, E. Favoino, J. Gutberlet, S. Baulch, M. E. Atreya, D. Fischer, K. K. He, M. M. Petit, U. Rashid Sumaila, E. Neil, M. V. Bernhofen, K. Lawrence and J. E. Palardy, Evaluating scenarios toward zero plastic pollution, *Science*, 2020, **369**, 1455–1461.
- 9 V. Yadav, M. A. Sherly, P. Ranjan, R. O. Tinoco, A. Boldrin, A. Damgaard and A. Laurent, Framework for quantifying environmental losses of plastics from landfills, *Resour., Conserv. Recycl.*, 2020, **161**, 104914.
- 10 X. Fei, Y. Guo, Y. Wang, M. Fang, K. Yin and H. He, The long-term fates of land-disposed plastic waste, *Nat. Rev. Earth Environ.*, 2022, **3**, 733–735.
- 11 K. Zhang, A. H. Hamidian, A. Tubić, Y. Zhang, J. K. H. Fang, C. Wu and P. K. S. Lam, Understanding plastic degradation and microplastic formation in the environment: A review, *Environ. Pollut.*, 2021, **274**, 116554.
- 12 Y. K. Song, S. H. Hong, M. Jang, G. M. Han, S. W. Jung and W. J. Shim, Combined Effects of UV Exposure Duration and Mechanical Abrasion on Microplastic Fragmentation by Polymer Type, *Environ. Sci. Technol.*, 2017, **51**, 4368–4376.
- 13 J. Gigault, B. Pedrono, B. Maxit and A. Ter Halle, Marine plastic litter: the unanalyzed nano-fraction, *Environ. Sci.: Nano*, 2016, **3**, 346–350.
- 14 M. Oliveira, M. Almeida and I. Miguel, A micro(nano)plastic boomerang tale: A never ending story?, *TrAC, Trends Anal. Chem.*, 2019, **112**, 196–200.
- 15 B. Chae, S. Oh and D. G. Lee, Is 5 mm still a good upper size boundary for microplastics in aquatic environments? Perspectives on size distribution and toxicological effects, *Mar. Pollut. Bull.*, 2023, **196**, 115591.
- 16 P. Merdy, F. Delpy, A. Bonneau, S. Villain, L. Iordachescu, J. Vollertsen and Y. Lucas, Nanoplastic production procedure for scientific purposes: PP, PVC, PE-LD, PE-HD, and PS, *Heliyon*, 2023, **9**(8), e18387.
- 17 N. B. Hartmann, T. Hüffer, R. C. Thompson, M. Hassellöv, A. Verschoor, A. E. Daugaard, S. Rist, T. Karlsson, N. Brennholt, M. Cole, M. P. Herrling, M. C. Hess, N. P. Ivleva, A. L. Lusher and M. Wagner, Are We Speaking the Same Language? Recommendations for a Definition and Categorization Framework for Plastic Debris, *Environ. Sci. Technol.*, 2019, **53**, 1039–1047.
- 18 European Commission and Directorate-General for Research and Innovation, *Nanoplastics – State of knowledge and environmental and human health impacts*, Publications Office of the European Union, 2023.
- 19 International Organization for Standardization, *Plastics - Environmental aspects - State of knowledge and methodologies (ISO Standard No. 21960:2020)*, 2020.
- 20 World Health Organization (WHO), *Dietary and inhalation exposure to nano- and microplastic particles and potential implications for human health*, 2022.
- 21 M. Bergmann, F. Collard, J. Fabres, G. W. Gabrielsen, J. F. Provencher, C. M. Rochman, E. van Seville and M. B. Tekman, Plastic pollution in the Arctic, *Nat. Rev. Earth Environ.*, 2022, **3**, 323–337.
- 22 S. Abbasi, A. Turner, M. Hoseini and H. Amiri, Microplastics in the Lut and Kavir Deserts, Iran, *Cite This, Environ. Sci. Technol.*, 2021, **55**, 6000.
- 23 E. Bergami, E. Rota, T. Caruso, G. Birarda, L. Vaccari and I. Corsi, Plastics everywhere: first evidence of polystyrene fragments inside the common Antarctic collembolan *Cryptopygus antarcticus*, *Biol. Lett.*, 2020, **16**(6), 20200093.
- 24 S. Allen, D. Allen, V. R. Phoenix, G. Le Roux, P. Durántez Jiménez, A. Simonneau, S. Binet and D. Galop, Atmospheric transport and deposition of microplastics in a remote mountain catchment, *Nat. Geosci.*, 2019, **12**, 339–344.
- 25 S. Chiba, H. Saito, R. Fletcher, T. Yogi, M. Kayo, S. Miyagi, M. Ogido and K. Fujikura, Human footprint in the abyss: 30 year records of deep-sea plastic debris, *Mar. Policy*, 2018, **96**, 204–212.
- 26 O. S. Alimi, J. Farner Budarz, L. M. Hernandez and N. Tufenkji, Microplastics and Nanoplastics in Aquatic Environments: Aggregation, Deposition, and Enhanced Contaminant Transport, *Environ. Sci. Technol.*, 2018, **52**, 1704–1724.
- 27 B. Kuizenga, P. F. Tasseront, K. Wendt-Potthoff and T. H. M. van Emmerik, From source to sea: Floating macroplastic transport along the Rhine river, *Front. Environ. Sci.*, 2023, **11**, 1180872.
- 28 V. S. Koutnik, J. Leonard, S. Alkidim, F. J. DePrima, S. Ravi, E. M. V. Hoek and S. K. Mohanty, Distribution of microplastics in soil and freshwater environments: Global analysis and framework for transport modeling, *Environ. Pollut.*, 2021, **274**, 116552.
- 29 D. Allen, S. Allen, S. Abbasi, A. Baker, M. Bergmann, J. Brahney, T. Butler, R. A. Duce, S. Eckhardt, N. Evangeliou, T. Jickells, M. Kanakidou, P. Kershaw, P. Laj, J. Levermore, D. Li, P. Liss, K. Liu, N. Mahowald, P. Masque, D. Materić, A. G. Mayes, P. McGinnity, I. Osvath, K. A. Prather, J. M. Prospero, L. E. Revell, S. G. Sander, W. J. Shim, J. Slade, A. Stein, O. Tarasova and S. Wright, Microplastics and nanoplastics in the marine-atmosphere environment, *Nat. Rev. Earth Environ.*, 2022, **3**, 393–405.
- 30 N. Evangeliou, H. Grythe, Z. Klimont, C. Heyes, S. Eckhardt, S. Lopez-Aparicio and A. Stohl, Atmospheric transport is a major pathway of microplastics to remote regions, *Nat. Commun.*, 2020, **11**, 3381.
- 31 A. Ragusa, A. Svelato, C. Santacroce, P. Catalano, V. Notarstefano, O. Carnevali, F. Papa, M. C. A. Rongioletti, F. Baiocco, S. Draghi, E. D'Amore, D. Rinaldo, M. Matta and E. Giorgini, Plasticenta: First evidence of microplastics in human placenta, *Environ. Int.*, 2021, **146**, 106274.
- 32 H. A. Leslie, M. J. M. van Velzen, S. H. Brandsma, A. D. Vethaak, J. J. Garcia-Vallejo and M. H. Lamoree, Discovery and quantification of plastic particle pollution in human blood, *Environ. Int.*, 2022, **163**, 107199.
- 33 L. C. Jenner, J. M. Rotchell, R. T. Bennett, M. Cowen, V. Tentzeris and L. R. Sadofsky, Detection of microplastics in human lung tissue using μ FTIR spectroscopy, *Sci. Total Environ.*, 2022, **831**, 154907.
- 34 P. Schwabl, S. Koppel, P. Konigshofer, T. Bucsics, M. Trauner, T. Reiberger and B. Liebmann, Detection of



- various microplastics in human stool: A prospective case series, *Ann. Intern. Med.*, 2019, **171**, 453–457.
- 35 S. L. Wright and F. J. Kelly, Plastic and Human Health: A Micro Issue?, *Environ. Sci. Technol.*, 2017, **51**, 6634–6647.
 - 36 European Commission and Directorate-General for Research and Innovation, *Environmental and health risks of microplastic pollution*, Publications Office of the European Union, 2019.
 - 37 EFSA Panel on Contaminants in the Food Chain (CONTAM), Statement on the presence of microplastics and nanoplastics in food, with particular focus on seafood, *EFSA J.*, 2016, **14**(6), e04501.
 - 38 O. O. Fadare, B. Wan, L.-H. Guo and L. Zhao, Microplastics from consumer plastic food containers: Are we consuming it?, *Chemosphere*, 2020, **253**, 126787.
 - 39 Md. I. Muhib, Md. K. Uddin, Md. M. Rahman and G. Malafaia, Occurrence of microplastics in tap and bottled water, and food packaging: A narrative review on current knowledge, *Sci. Total Environ.*, 2023, **865**, 161274.
 - 40 B. E. Oßmann, G. Sarau, H. Holtmannspötter, M. Pischetsrieder, S. H. Christiansen and W. Dicke, Small-sized microplastics and pigmented particles in bottled mineral water, *Water Res.*, 2018, **141**, 307–316.
 - 41 S. Kernchen, M. G. J. Löder, F. Fischer, D. Fischer, S. R. Moses, C. Georgi, A. C. Nölscher, A. Held and C. Laforsch, Airborne microplastic concentrations and deposition across the Weser River catchment, *Sci. Total Environ.*, 2022, **818**, 151812.
 - 42 Y. Geng, Z. Zhang, W. Zhou, X. Shao, Z. Li and Y. Zhou, Individual Exposure to Microplastics through the Inhalation Route: Comparison of Microplastics in Inhaled Indoor Aerosol and Exhaled Breath Air, *Environ. Sci. Technol. Lett.*, 2023, **10**, 464–470.
 - 43 L. Rahman, G. Mallach, R. Kulka and S. Halappanavar, Microplastics and nanoplastics science: collecting and characterizing airborne microplastics in fine particulate matter, *Nanotoxicology*, 2021, **15**, 1253–1278.
 - 44 D. O'Connor, S. Pan, Z. Shen, Y. Song, Y. Jin, W.-M. Wu and D. Hou, Microplastics undergo accelerated vertical migration in sand soil due to small size and wet-dry cycles, *Environ. Pollut.*, 2019, **249**, 527–534.
 - 45 K. Tanaka, Y. Takahashi, H. Kuramochi, M. Osako, S. Tanaka and G. Suzuki, Preparation of Nanoscale Particles of Five Major Polymers as Potential Standards for the Study of Nanoplastics, *Small*, 2021, **17**, 2105781.
 - 46 W. S. Lee, H. Kim, Y. Sim, T. Kang and J. Jeong, Fluorescent Polypropylene Nanoplastics for Studying Uptake, Biodistribution, and Excretion in Zebrafish Embryos, *ACS Omega*, 2022, **7**, 2467–2473.
 - 47 J. Seghers, E. A. Stefaniak, R. La Spina, C. Cella, D. Mehn, D. Gilliland, A. Held, U. Jacobsson and H. Emteborg, Preparation of a reference material for microplastics in water-evaluation of homogeneity, *Anal. Bioanal. Chem.*, 2022, 385–397.
 - 48 G. Balakrishnan, M. Déniel, T. Nicolai, C. Chassenieux and F. Lagarde, Towards more realistic reference microplastics and nanoplastics: preparation of polyethylene micro/nanoparticles with a biosurfactant, *Environ. Sci.: Nano*, 2019, **6**, 315.
 - 49 J. Hildebrandt and A. F. Thünemann, Aqueous Dispersions of Polypropylene: Toward Reference Materials for Characterizing Nanoplastics, *Macromol. Rapid Commun.*, 2023, 2200874.
 - 50 S. Ducoli, S. Federici, R. Nicsanu, A. Zandrini, C. Marchesi, L. Paolini, A. Radeghieri, P. Bergese and L. E. Depero, A different protein corona cloaks “true-to-life” nanoplastics with respect to synthetic polystyrene nanobeads, *Environ. Sci.: Nano*, 2022, **9**(4), 1414–1426.
 - 51 J. R. Peller, S. P. Mezyk, S. Shidler, J. Castleman, S. Kaiser, R. F. Faulkner, C. D. Pilgrim, A. Wilson, S. Martens and G. P. Horne, Facile nanoplastics formation from macro and microplastics in aqueous media, *Environ. Pollut.*, 2022, **313**, 120171.
 - 52 National Institute of Standards and Technology, SRM Definitions, <https://www.nist.gov/srm/srm-definitions>, (accessed 30 August 2024).
 - 53 International Organization for Standardization, ISO Guide 30 (2015): Reference materials - Selected terms and definitions, 2015.
 - 54 International Organization for Standardization, ISO 33405 (2024): Reference materials - Approaches for characterization and assessment of homogeneity and stability, 2024.
 - 55 International Organization for Standardization, ISO 33401 (2024): Reference materials - Contents of certificates, labels and accompanying documentation, 2024.
 - 56 E. L. Romsos, C. R. Steffen and P. M. Vallone, Development of a research grade test material for supporting community-wide validation efforts, Washington D.C., 2022.
 - 57 S. Lin, H. Zhang, C. Wang, X.-L. Su, Y. Song, P. Wu, Z. Yang, M.-H. Wong, Z. Cai and C. Zheng, Metabolomics Reveal Nanoplastic-Induced Mitochondrial Damage in Human Liver and Lung Cells, *Environ. Sci. Technol.*, 2022, **56**, 12483–12493.
 - 58 P. Wick, A. Malek, P. Manser, D. Meili, X. Maeder-Althaus, L. Diener, P.-A. Diener, A. Zisch, H. F. Krug and U. von Mandach, Barrier Capacity of Human Placenta for Nanosized Materials, *Environ. Health Perspect.*, 2010, **118**, 432–436.
 - 59 A. Tavakolpournegari, B. Annangi, A. Villacorta, G. Banaei, J. Martin, S. Pastor, R. Marcos and A. Hernández, Hazard assessment of different-sized polystyrene nanoplastics in hematopoietic human cell lines, *Chemosphere*, 2023, **325**, 138360.
 - 60 M. Tamayo-Belda, J. J. Vargas-Guerrero, K. Martín-Betancor, G. Pulido-Reyes, M. González-Pleiter, F. Leganés, R. Rosal and F. Fernández-Piñas, Understanding nanoplastic toxicity and their interaction with engineered cationic nanoplastics in microalgae by physiological and proteomic approaches, *Environ. Sci.: Nano*, 2021, **8**, 2277–2296.
 - 61 O. Pikuda, E. G. Xu, D. Berk and N. Tufenkji, Toxicity Assessments of Micro- and Nanoplastics Can Be Confounded by Preservatives in Commercial Formulations, *Environ. Sci. Technol. Lett.*, 2019, **6**, 21–25.



- 62 M. Heinlaan, K. Kasemets, V. Aruoja, I. Blinova, O. Bondarenko, A. Lükjanova, A. Khosrovyan, I. Kurvet, M. Pullerits, M. Sihtmäe, G. Vasiliev, H. Vija and A. Kahru, Hazard evaluation of polystyrene nanoplastic with nine bioassays did not show particle-specific acute toxicity, *Sci. Total Environ.*, 2020, **707**, 136073.
- 63 E. J. Petersen, A. C. Barrios, T. B. Henry, M. E. Johnson, A. A. Koelmans, A. R. Montoro Bustos, J. Matheson, M. Roesslein, J. Zhao and B. Xing, Potential Artifacts and Control Experiments in Toxicity Tests of Nanoplastic and Microplastic Particles, *Environ. Sci. Technol.*, 2022, **56**, 15192–15206.
- 64 T. F. Lins, A. M. O'Brien, T. Kose, C. M. Rochman and D. Sinton, Toxicity of nanoplastics to zooplankton is influenced by temperature, salinity, and natural particulate matter, *Environ. Sci.: Nano*, 2022, **9**, 2678–2690.
- 65 L. A. Parker, E. M. Höppener, E. F. van Amelrooij, S. Henke, I. M. Kooter, K. Grigoriadi, M. G. A. Nooijens, A. M. Brunner and A. Boersma, Protocol for the production of micro- and nanoplastic test materials, *Microplast. Nanoplast.*, 2023, **3**, 10.
- 66 Y. Ji, L. Chen, Y. Wang, J. Zhang, Y. Yu, M. Wang, X. Wang, W. Liu, B. Yan, L. Xiao, X. Song, C. Lv and L. Chen, Realistic Nanoplastics Induced Pulmonary Damage via the Crosstalk of Ferritinophagy and Mitochondrial Dysfunction, *ACS Nano*, 2024, **18**, 16790–16807.
- 67 I. Inkielewicz-Stepniak, L. Tajber, G. Behan, H. Zhang, M. W. Radomski, C. Medina and M. J. Santos-Martinez, The role of mucin in the toxicological impact of polystyrene nanoparticles, *Materials*, 2018, **11**(5), 724.
- 68 M. Sultan, X.-Y. Wei, J.-J. Duan, B.-F. Zhang, M.-F. Wu, Z.-X. Cai and D.-S. Pei, Comparative toxicity of polystyrene, polypropylene, and polyethylene nanoplastics on *Artemia franciscana* nauplii: a multidimensional assessment, *Environ. Sci.: Nano*, 2024, **11**, 1070–1084.
- 69 M. Auguste, T. Balbi, A. Miglioli, S. Alberti, S. Prandi, R. Narizzano, A. Salis, G. Damonte and L. Canesi, Comparison of Different Commercial Nanopolystyrenes: Behavior in Exposure Media, Effects on Immune Function and Early Larval Development in the Model Bivalve *Mytilus galloprovincialis*, *Nanomaterials*, 2021, **11**(12), 3291.
- 70 Bundesanstalt für Materialforschung und -prüfung (BAM), BAM Referenzmaterialien - Polymermaterialien, https://webshop.bam.de/webshop_de/referenzmaterialien/polymermaterialien.html, (accessed 3 September 2024).
- 71 National Institute of Standards and Technology (NIST), Reference Materials for Plastic Pollution Measurement Science, <https://www.nist.gov/programs-projects/reference-materials-plastic-pollution-measurement-science>, (accessed 3 September 2024).
- 72 Hawai'i Pacific University (HPU), *Polymer Kit 1.0*, <https://www.hpu.edu/cnscs/cmdr/products-and-services.html>, (accessed 3 September 2024).
- 73 CD Bioparticles, CD Bioparticles - Polymer Particles, <https://www.cd-bioparticles.com/product/polymer-particles-list-172.html>, (accessed 3 September 2024).
- 74 J. Ali, K. Pramod, Ma. Tahir, N. Charoo and S. Ansari, Pharmaceutical product development: A quality by design approach, *Int. J. Pharm. Invest.*, 2016, **6**, 129.
- 75 A. G. Rodríguez-Hernández, J. Alejandro Muñoz-Tabares, J. Cristobal Aguilar-Guzmán and R. Vazquez-Duhalt, A novel and simple method for polyethylene terephthalate (PET) nanoparticle production, *Environ. Sci.: Nano*, 2019, **6**(7), 2031–2036.
- 76 R. Christoph, B. Schmidt, U. Steinberner, W. Dilla and R. Karinen, Glycerol, in *Ullmann's Encyclopedia of Industrial Chemistry*, 2006.
- 77 S. S. Gaikwad, J. O. Morales, N. B. Lande, J. Catalán-Figueroa, U. D. Laddha and S. J. Kshirsagar, Exploring paediatric oral suspension development: Challenges, requirements, and formulation advancements, *Int. J. Pharm.*, 2024, **657**, 124169.
- 78 L. R. Morrison, Glycerol, in *Kirk-Othmer Encyclopedia of Chemical Technology*, 2000.
- 79 Pharmaceutical Press and American Pharmacists Association, *Handbook of Pharmaceutical Excipients*, *Handbook of Pharmaceutical Excipients*, Pharmaceutical Press & American Pharmacists Association, London, 6th edn, 2009.
- 80 M. S. B. Frank, M. C. Nahata and M. D. Hilty, Glycerol: A Review of Its Pharmacology, Pharmacokinetics, Adverse Reactions, and Clinical Use, *Pharmacotherapy*, 1981, **1**, 147–160.
- 81 DAC/NRF-KommissionABDA and Bundesvereinigung Deutscher Apothekerverbände e. V., Deutscher Arzneimittel-Codex®/Neues Rezeptur-Formularium® (DAC/NRF), in DAC/NRF, Deutschen Apotheker Verlag, 2024/1, 2024.
- 82 D. S. Wishart, C. Knox, A. C. Guo, D. Cheng, S. Shrivastava, D. Tzur, B. Gautam and M. Hassanali, DrugBank: a knowledgebase for drugs, drug actions and drug targets, *Nucleic Acids Res.*, 2008, **36**, D901–D906.
- 83 R. Scherließ, The MTT assay as tool to evaluate and compare excipient toxicity in vitro on respiratory epithelial cells, *Int. J. Pharm.*, 2011, **411**, 98–105.
- 84 D. S. Achilias, A. A. Giannoulis, A. G. Z. Papageorgiou, Á. A. Giannoulis and G. Z. Papageorgiou, Recycling of polymers from plastic packaging materials using the dissolution-reprecipitation technique, *Polym. Bull.*, 2009, **63**, 449–465.
- 85 K. Tanaka, H. Kuramochi, K. Maeda, Y. Takahashi, M. Osako and G. Suzuki, Size-Controlled Preparation of Polyethylene Nanoplastic Particles by Nanoprecipitation and Insights into the Underlying Mechanisms, *ACS Omega*, 2023, **8**, 14470–14477.
- 86 R. B. Schefer, A. Armanious and D. M. Mitrano, Eco-Corona Formation on Plastics: Adsorption of Dissolved Organic Matter to Pristine and Photochemically Weathered Polymer Surfaces, *Environ. Sci. Technol.*, 2023, **57**, 14707–14716.
- 87 I. Ali, X. Tan, C. Peng, I. Naz, Y. Zhang, A. Hernández, R. Marcos, R. Pervez, Z. Duan and Y. Ruan, Eco- and bio-corona-based microplastics and nanoplastics complexes in the environment: Modulations in the toxicological behavior of plastic particles and factors affecting, *Process Saf. Environ. Prot.*, 2024, **187**, 356–375.



- 88 Food and Drug Administration, *Pharmaceutical Microbiology Manual*, 2020.
- 89 Ph. Eur. 11, 4.5.4.2.1 Plattengussverfahren, in European Pharmacopoeia 11, 2023.
- 90 B. W. Neun and M. A. Dobrovolskaia, NCL Method STE-1.1: Detection and Quantification of Gram Negative Bacterial Endotoxin Contamination in Nanoparticle Formulations by End Point Chromogenic LAL Assay, <https://ncl.cancer.gov/resources/assay-cascade-protocols>, DOI: [10.17917/5WSQ-7X78](https://doi.org/10.17917/5WSQ-7X78).
- 91 Corning Inc., Endotoxins and Cell Culture - Technical Guide.
- 92 Y. Li, Z. Shi, I. Radauer-Preiml, A. Andosch, E. Casals, U. Luetz-Meindl, M. Cobaleda, Z. Lin, M. Jaber-Douraki, P. Italiani, J. Horejs-Hoeck, M. Himly, N. A. Monteiro-Riviere, A. Duschl, V. F. Puentes and D. Boraschi, Bacterial endotoxin (lipopolysaccharide) binds to the surface of gold nanoparticles, interferes with biocorona formation and induces human monocyte inflammatory activation, *Nanotoxicology*, 2017, **11**, 1157–1175.
- 93 J. M. Costello and S. T. Bowden, The temperature variation of orthobaric density difference in liquid-vapour systems. III. Alcohols, *Recl. Trav. Chim. Pays-Bas*, 1958, **77**, 36–46.
- 94 S. T. Stern, P. P. Adiseshaiah and T. P. Potter, NCL Method GTA-1: LLC-PK1 Kidney Cytotoxicity Assay, <https://ncl.cancer.gov/resources/assay-cascade-protocols>, DOI: [10.17917/Q6EC-XC97](https://doi.org/10.17917/Q6EC-XC97).
- 95 D. Wang, Q. Sun, M. J. Hokkanen, C. Zhang, F.-Y. Lin, Q. Liu, S.-P. Zhu, T. Zhou, Q. Chang, B. He, Q. Zhou, L. Chen, Z. Wang, R. H. A. Ras and X. Deng, Design of robust superhydrophobic surfaces, *Nature*, 2020, **582**, 55–59.
- 96 M. Yamamoto, N. Nishikawa, H. Mayama, Y. Nonomura, S. Yokojima, S. Nakamura and K. Uchida, Theoretical Explanation of the Lotus Effect: Superhydrophobic Property Changes by Removal of Nanostructures from the Surface of a Lotus Leaf, *Langmuir*, 2015, **31**, 7355–7363.
- 97 K. Aljoumaa and M. Abboudi, Physical ageing of polyethylene terephthalate under natural sunlight: correlation study between crystallinity and mechanical properties, *Appl. Phys. A: Mater. Sci. Process.*, 2015, **122**, 6.
- 98 A. Rjeb, L. Tajounte, M. C. El Idrissi, S. Letarte, A. Adnot, D. Roy, Y. Claire, A. Périchaud and J. Kaloustian, IR spectroscopy study of polypropylene natural aging, *J. Appl. Polym. Sci.*, 2000, **77**, 1742–1748.
- 99 Y. Bide, M. A. Fashapoyeh and S. Shokrollahzadeh, Structural investigation and application of Tween 80-choline chloride self-assemblies as osmotic agent for water desalination, *Sci. Rep.*, 2021, **11**, 17068.
- 100 Z. Weiszhar, J. Czucz, C. Révész, L. Rosivall, J. Szebeni and Z. Rozsnyay, Complement activation by polyethoxylated pharmaceutical surfactants: Cremophor-EL, Tween-80 and Tween-20, *Eur. J. Pharm. Sci.*, 2012, **45**, 492–498.
- 101 A. Rawle, Basic principles of particle size analysis, *Surf. Coat. Int., Part A*, 2003, **86**(2), 58–65.
- 102 Y. Li, P. Italiani, E. Casals, N. Tran, V. F. Puentes and D. Boraschi, Optimising the use of commercial LAL assays for the analysis of endotoxin contamination in metal colloids and metal oxide nanoparticles, *Nanotoxicology*, 2015, **9**, 462–473.
- 103 G. J. Oostingh, E. Casals, P. Italiani, R. Colognato, R. Stritzinger, J. Ponti, T. Pfaller, Y. Kohl, D. Ooms, F. Favilli, H. Leppens, D. Lucchesi, F. Rossi, I. Nelissen, H. Thielecke, V. F. Puentes, A. Duschl and D. Boraschi, Problems and challenges in the development and validation of human cell-based assays to determine nanoparticle-induced immunomodulatory effects, *Part. Fibre Toxicol.*, 2011, **8**, 8.
- 104 Y. Li, M. Fujita and D. Boraschi, Endotoxin Contamination in Nanomaterials Leads to the Misinterpretation of Immunosafety Results, *Front. Immunol.*, 2017, **8**, 472.
- 105 C. Wunderlich, S. Schumacher and M. Kietzmann, Pyrogen detection methods: Comparison of bovine whole blood assay (bWBA) and monocyte activation test (MAT), *BMC Pharmacol. Toxicol.*, 2014, **15**, 50.
- 106 M. Grauso, A. Lan, M. Andriamihaja, F. Bouillaud and F. Blachier, Hyperosmolar environment and intestinal epithelial cells: impact on mitochondrial oxygen consumption, proliferation, and barrier function in vitro, *Sci. Rep.*, 2019, **9**, 11360.
- 107 A. Guyot and J. W. Hanrahan, ATP release from human airway epithelial cells studied using a capillary cell culture system, *J. Physiol.*, 2002, **545**, 199–206.
- 108 M. D. Gundersen, K. B. Larsen, K. M. Johnsen, R. Goll, J. Florholmen and G. Haraldsen, Hypo-osmotic stress induces the epithelial alarmin IL-33 in the colonic barrier of ulcerative colitis, *Sci. Rep.*, 2022, **12**, 11550.
- 109 A. Miermont, S. W. L. Lee, G. Adriani and R. D. Kamm, Quantitative screening of the effects of hyper-osmotic stress on cancer cells cultured in 2- or 3-dimensional settings, *Sci. Rep.*, 2019, **9**, 13782.
- 110 J. D. Finan and F. Guilak, The effects of osmotic stress on the structure and function of the cell nucleus, *J. Cell. Biochem.*, 2010, **109**, 460–467.
- 111 H. M. Taïeb, D. S. Garske, J. Contzen, M. Gossen, L. Bertinetti, T. Robinson and A. Cipitria, Osmotic pressure modulates single cell cycle dynamics inducing reversible growth arrest and reactivation of human metastatic cells, *Sci. Rep.*, 2021, **11**, 13455.
- 112 V. Dhaka, S. Singh, A. G. Anil, T. S. Sunil Kumar Naik, S. Garg, J. Samuel, M. Kumar, P. C. Ramamurthy and J. Singh, Occurrence, toxicity and remediation of polyethylene terephthalate plastics: A review, *Environ. Chem. Lett.*, 2022, **20**, 1777–1800.
- 113 R. Ahmad Khanbeigi, A. Kumar, F. Sadouki, C. Lorenz, B. Forbes, L. A. Dailey and H. Collins, The delivered dose: Applying pharmacokinetics to in vitro investigations of nanoparticle internalization by macrophages, *J. Controlled Release*, 2012, **162**, 259–266.
- 114 P. M. Hinderliter, K. R. Minard, G. Orr, W. B. Chrisler, B. D. Thrall, J. G. Pounds and J. G. Teeguarden, ISDD: A computational model of particle sedimentation, diffusion and target cell dosimetry for in vitro toxicity studies, *Part. Fibre Toxicol.*, 2010, **7**, 36.



- 115 G. DeLoid, J. M. Cohen, T. Darrah, R. Derk, L. Rojanasakul, G. Pyrgiotakis, W. Wohlleben and P. Demokritou, Estimating the effective density of engineered nanomaterials for in vitro dosimetry, *Nat. Commun.*, 2014, **5**, 3514.
- 116 International Organization for Standardization, *Biological evaluation of medical devices - Part 5: Tests for in vitro cytotoxicity (ISO Standard No. 10993:2009)*, 2009.
- 117 V. Tolardo, D. Magri, F. Fumagalli, D. Cassano, A. Athanassiou, D. Fragouli and S. Gioria, In Vitro High-Throughput Toxicological Assessment of Nanoplastics, *Nanomaterials*, 2022, **12**(12), 1947.
- 118 S. Yang, Y. Cheng, Z. Chen, T. Liu, L. Yin, Y. Pu and G. Liang, In vitro evaluation of nanoplastics using human lung epithelial cells, microarray analysis and co-culture model, *Ecotoxicol. Environ. Saf.*, 2021, **226**, 112837.
- 119 L. Schröter and N. Ventura, Nanoplastic Toxicity: Insights and Challenges from Experimental Model Systems, *Small*, 2022, **18**, 2201680.
- 120 International Organization for Standardization, *ISO Guide 35 (2017): Reference materials - guidance for characterisation and assessment of homogeneity and stability*, 2017.
- 121 C. Veclin, C. Desmet, A. Pradel, A. Valsesia, J. Ponti, H. El Hadri, T. Maupas, V. Pellerin, J. Gigault, B. Grassl and S. Reynaud, Effect of the Surface Hydrophobicity-Morphology-Functionality of Nanoplastics on Their Homoaggregation in Seawater, *ACS ES&T Water*, 2022, **2**, 88–95.
- 122 L. Schröter and N. Ventura, Nanoplastic Toxicity: Insights and Challenges from Experimental Model Systems, *Small*, 2022, **18**, 2201680.

